Stem Cell Reports
Article

OPEN ACCESS

X Chromosome of Female Cells Shows Dynamic Changes in Status during Human Somatic Cell Reprogramming

Kun-Yong Kim,[1] Eriona Hysolli,[1] Yoshiaki Tanaka,[1] Brandon Wang,[2] Yong-Wook Jung,[1,3] Xinghua Pan,[1] Sherman Morton Weissman,[1] and In-Hyun Park[1,*]

[1]Department of Genetics, Yale Stem Cell Center, Yale School of Medicine, 10 Amistad, 201B, New Haven, CT 06520, USA
[2]Molecular, Cellular and Developmental Biology, Yale University, 219 Prospect Street, New Haven, CT 06511, USA
[3]Department of Obstetrics and Gynecology, CHA Gangnam Medical Center, CHA University, Seoul 135-080, Republic of Korea
*Correspondence: inhyun.park@yale.edu
http://dx.doi.org/10.1016/j.stemcr.2014.04.003

SUMMARY

Induced pluripotent stem cells (iPSCs) acquire embryonic stem cell (ESC)-like epigenetic states, including the X chromosome. Previous studies reported that human iPSCs retain the inactive X chromosome of parental cells, or acquire two active X chromosomes through reprogramming. Most studies investigated the X chromosome states in established human iPSC clones after completion of reprogramming. Thus, it is still not fully understood when and how the X chromosome reactivation occurs during reprogramming. Here, we report a dynamic change in the X chromosome state throughout reprogramming, with an initial robust reactivation of the inactive X chromosome followed by an inactivation upon generation of nascent iPSC clones. iPSCs with two active X chromosomes or an eroded X chromosome arise in passaging iPSCs. These data provide important insights into the plasticity of the X chromosome of human female iPSCs and will be crucial for the future application of such cells in cell therapy and X-linked disease modeling.

INTRODUCTION

Expression of a defined set of transcription factors (OCT4, SOX2, KLF4, and c-MYC) reprograms human somatic cells to a pluripotent state, generating induced pluripotent stem cells (iPSCs) (Park et al., 2008b; Takahashi et al., 2007; Yu et al., 2007). iPSCs are similar to embryonic stem cells (ESCs) and are capable of indefinite self-renewal and differentiation into cells of all three germ layers. iPSCs also maintain the genomic composition of parental somatic cells and thus are considered as autologous cellular resources that are critical for cell therapy and in vitro disease modeling (Park et al., 2008a; Wu and Hochedlinger, 2011). Detailed genetic and epigenetic comparisons between iPSCs and ESCs, however, have shown that they are close but not identical (Chin et al., 2009). Reprogramming leaves reprogramming-specific epigenetic marks and produces copy number variation (Hussein et al., 2011; Lister et al., 2011). In addition, de novo mutations seem to accompany reprogramming and cause genetic alterations in iPSCs, although more in-depth analyses are needed before we can draw definite conclusions regarding the genetic changes in reprogramming (Abyzov et al., 2012; Gore et al., 2011).

Reprogramming affects the X chromosome status in female cells. During early development, one of the active X chromosomes in the inner cell mass (ICM) cells of the blastocyst undergoes random X chromosome inactivation (XCI) when ICM cells differentiate into epiblast cells (Mak et al., 2004). Only cells that are committed to developing as primordial germ cells (PGCs) start to reactivate the inactive X chromosome during migration to the genital ridge. In contrast, somatic cells maintain the inactive X chromosome throughout their life (de Napoles et al., 2007). Murine ESCs derived from ICM cells are considered to be in a naive state, and there are two active X chromosomes in female ESCs (Hanna et al., 2010). The X chromosome status in murine female iPSCs is indistinguishable from that in murine ESCs. Reprogramming activates the inactive X chromosome to produce iPSCs with two active X chromosomes (Maherali et al., 2007). Human ESCs are presumed to be derived from the epiblast cells of the embryo and have one inactive X chromosome. However, successful derivation of human ESCs with two active X chromosomes suggested that human ESCs are counterparts of ICM cells as well, but are prone to undergo XCI unless they are maintained in a pristine physiological condition, including a hypoxic oxygen concentration and no oxidative stress (Diaz Perez et al., 2012; Lengner et al., 2010). Thus, most human ESCs were reported to carry only one active X chromosome. In-depth studies on female human ESCs categorized them into three classes according to their X chromosome status (Kim et al., 2011; Lessing et al., 2013). Class I female human ESCs have two active X chromosomes, like murine ESCs, and show neither H3K27me3 nor *XIST* foci. When differentiated, class I ESCs undergo random XCI and form H3K27me3 foci and a *XIST* cloud. Spontaneous inactivation of one of the two X chromosomes in class I ESCs results in the formation of H3K27me3 and *XIST* foci, leading to the conversion of class I to class II cells. Class II ESCs maintain the inactive X chromosome after differentiation. However, the inactive X chromosome in class II ESCs is reversible and becomes

reactivated with treatment of HDAC inhibitors (Diaz Perez et al., 2012). Continuous long-term passaging of H3K27me3 foci-positive class II ESCs triggers them to become H3K27me3 foci-negative class III ESCs. Although they are negative for H3K27me3 foci and *XIST* expression, class III ESCs carry one inactive X chromosome whose status seems to be permanent, and do not show H3K27me3 foci upon differentiation (Diaz Perez et al., 2012). As in the case of human ESCs, female iPSCs seem to have only one active X chromosome because they retain the inactive X chromosome (Tchieu et al., 2010). However, some groups, including ours, have found that iPSCs with two active X chromosomes can be generated via reprogramming (Kim et al., 2011; Marchetto et al., 2010; Tomoda et al., 2012). Others found that reprogramming does not reactivate the inactive X chromosome, and instead the unstable inactive X chromosome undergoes epigenetic erosion, producing class III iPSCs (Mekhoubad et al., 2012). The female iPSCs that have lost *XIST* expression seem to be less desirable cells for cell therapy or disease modeling because *XIST* loss is highly correlated with upregulation of X-linked oncogenes, which leads to a high growth rate and poor differentiation (Anguera et al., 2012). A recent study showed that high expression of leukemia inhibitory factor (LIF) facilitates the derivation of iPSCs with two active X chromosomes (Tomoda et al., 2012). The difference in X chromosome status in iPSCs among different labs suggests that the X chromosome is not in a stable state in current culture conditions.

There are many X-linked diseases in females for which iPSC-based disease modeling and future cell therapies are readily applicable. Thus, information regarding X chromosome status during reprogramming and in established iPSCs is critical. Here, we set out to detail the change in X chromosome status that occurs during human female somatic cell reprogramming. Remarkably, we found that the change in the X chromosome is dynamic during reprogramming. Reprogramming at the early stage causes reactivation of the inactive X chromosome of the parental fibroblast, which does not seem to be permanent and rapidly becomes inactivated in the nascent iPSC colonies. The inactive X chromosome can be reactivated, eroded, or maintained during early passages in established iPSCs, producing class I, II, and III iPSCs that have different states of X chromosome. Our data suggest that the X chromosome status is not permanently fixed, but is plastic during human somatic cell reprogramming.

RESULTS

Reprogramming Changes the X Chromosome Status

In order to monitor changes in the inactive X chromosome state during female somatic cell reprogramming, we took advantage of a monoallelic D551-iPSCK1 clone that is derived from normal female Detroit 551 fibroblasts and has only one active X chromosome. We monitored the X chromosome status of the monoallelic D551-iPSCK1 clone by H3K27me3 staining and by performing a SNP analysis of X-linked genes (e.g., the TT allele in *GRPR*; Figure 1A). Differentiation in the D551-iPSCK1 cells was induced to produce dfD551-K1 fibroblast-like cells that maintained the specificity of X chromosome allelic gene expression, and expressed only the TT SNP of the *GRPR* gene. We then reprogrammed dfD551-K1 cells and derived ten clones of dfD551K1-iPSC lines, and examined the X chromosome status (Figure 1A; Figure S1A available online; Table 1). Two clones of dfD551K1-iPSC showed expression of the TT SNP *GRPR* of the parental fibroblasts (Tchieu et al., 2010). We found that six dfD551K1-iPSC clones expressed both AA and TT alleles of *GRPR* that may have acquired two active X chromosomes via X chromosome reactivation (XCR) during reprogramming (Tomoda et al., 2012). However, unexpectedly, two clones of dfD551K1-iPSC expressed *GRPR* with the AA allele. If the iPSC retains the inactive X chromosome state or reactivates the inactive X chromosome, iPSC clones expressing X-linked genes with the opposite SNP of the parental fibroblasts are not expected to be produced. We confirmed the X chromosome status of the dfD551K1-iPSC clones by examining the presence of H3K27me3 foci and *XIST* clouds, which are present in monoallelic clones and absent in biallelic clones (Figures 1B and 1C). We then compared the transcription of XCI-related genes and X-linked genes between mono- and biallelic dfD551K1-iPSC clones. iPSC lines without H3K27me3 foci showed lower expression of XCI-related *XIST*, *EZH2*, and *RNF12*, but showed higher expression of X-linked *MECP2* (methyl CpG-binding protein 2) and *HPRT* (hypoxanthine-guanine phosphoribosyl transferase), representing the absence of the inactive X chromosome (Figure S1B). These data suggest that the inactive X chromosome of fibroblasts may have undergone a reactivation and then a subsequent inactivation during reprogramming. Similarly, we differentiated monoallelic Rett syndrome (RTT) iPSC lines and generated fibroblast-like cells that expressed only one allele of the X-linked gene *MECP2* (dfRTT3-46m, dfRTT4-24w, and dfRTT5-34m). We generated clones of iPSCs from these fibroblast-like cells and examined the allelic expression of *MECP2*. As with the iPSC clones derived from dfD551-K1 cells, we found iPSC clones with the same allelic expression of *MECP2* as the parental fibroblasts, the opposite SNP, or both (Figures S1C–S1E; Table 1), further supporting our finding of X chromosome dynamics, including reactivation, during reprogramming.

In order to elucidate the dynamics of X chromosome during reprogramming, we traced the X chromosome status in cells undergoing reprogramming. Following

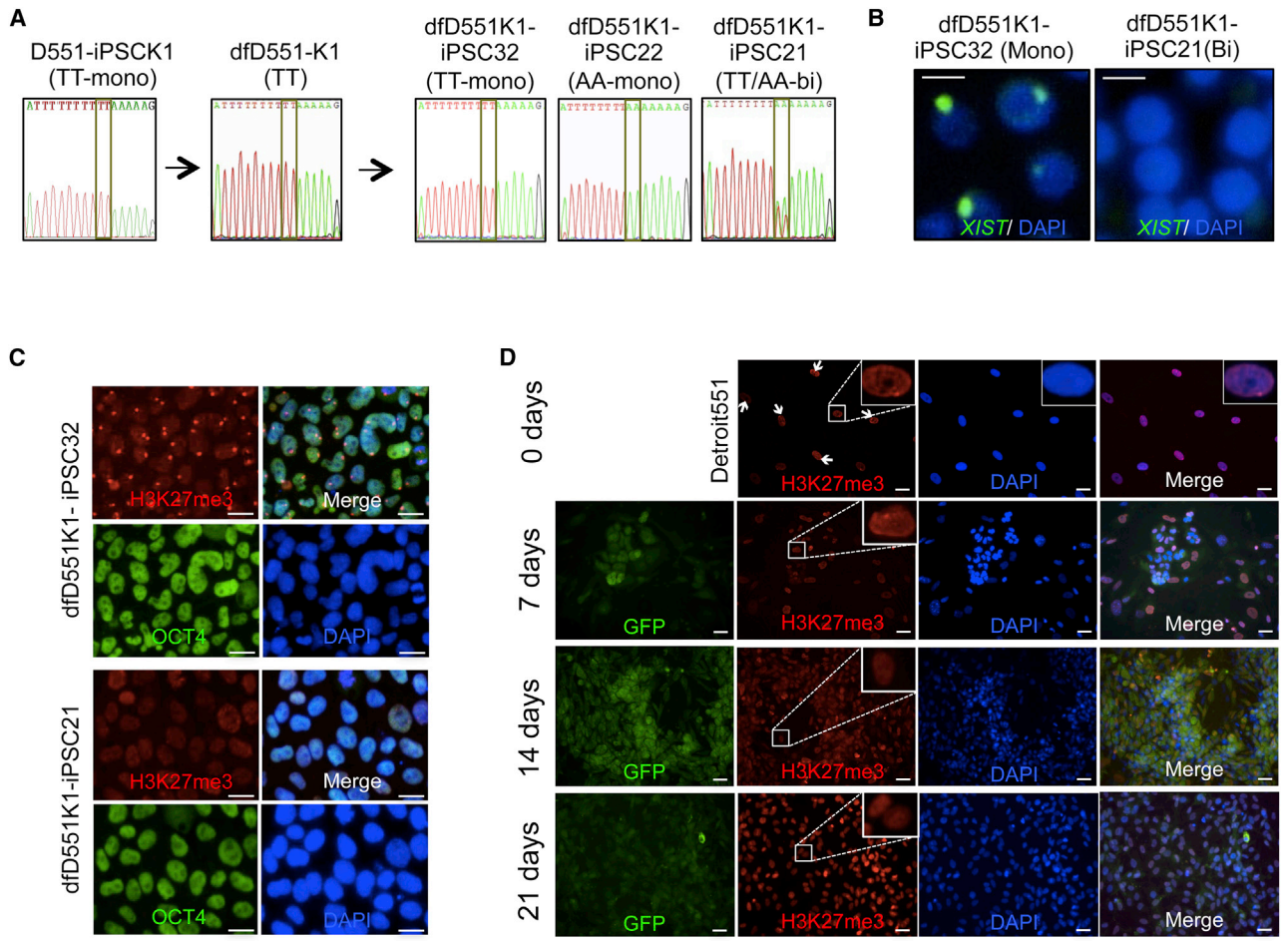

(legend on next page)

Table 1. Clonal Fibroblast Lines and the iPSC Clonal Lines Derived from Them

Parental Cells	Clonal Fibroblasts	SNP Gene	SNP (A/B) and Location	Secondary iPSC with A Allele	Secondary iPSC with A/B Allele	Secondary iPSC with B Alleles
D551-iPSCK1	dfD551-K1	*GRPR*	TT/AA at 2,411–2,412	2	6	2
6TG-iPSC3	df6TG-3	*GYG2*	C/T at 998	2	2	2
		GYG2	A/G at 1,127			
HAT-iPSC1	dfHAT-1	*GYG2*	C/T at 998	2	3	1
		GYG2	A/G at 1,127			
		MAOA	A/G at 4,100			
RTT3-iPSC-46m	dfRTT3-46m	*MECP2*	Del G at 705	4	3	2
RTT4-iPSC-24w	dfRTT4-24w	*MECP2*	C/T at 916	4	2	5
RTT5-iPSC-34m	dfRTT5-34m	*MECP2*	A/G at 1,461	2	4	3
fLNS HPRT$^{+/-}$	fLNS-6TG	*GYG2*	C/T at 998	4	3	2
		GYG2	A/G at 1,127			
		MAOA	A/G at 4,100			

Fibroblast-like cells were generated from monoallelic iPSCs by differentiation. fLNS-6TG fibroblasts resistant to 6TG or fLNS-HAT fibroblasts resistant to HAT were selected from LNS fibroblasts with 6TG treatment or HAT medium. Differentiated fibroblasts, fLNS-6TG, and fLNS-HAT have monoallelic expression of genes on the X chromosome. When induced for reprogramming, iPSC clones with the same allelic expression of X-linked genes of the parental fibroblasts, iPSC clones with the opposite allele, or both are produced.

reprogramming of Detroit 551 fibroblast, cells were fixed at 7, 14, and 21 days for analysis in X chromosome state. First, we examined the change in H3K27me3 foci, which is the most reliable marker for the presence of an inactive X chromosome (Plath et al., 2003). As reprogramming proceeded, the percentage of cells with H3K27me3 foci gradually decreased and became 7% at day 21 (Figures 1D and 1E). These data further support the notion that reprogramming reactivates the inactive X chromosome. We also found a gradual decrease of H3K27me3 foci-positive cells in three other primary fibroblast cell lines (RTT3, WI38, and IMR90; Figures S2A–S2C).

Next, we examined whether the expression of genes that are critical for XCI changes during reprogramming. We isolated total RNA in cells undergoing reprogramming at 10, 14, 21, and 28 days after reprogramming, and analyzed the expression of XCI-related and pluripotent genes (Figure S2D). *XIST* is a noncoding RNA whose expression and

Figure 1. Analysis of the X Chromosome Status of Female iPSC Lines Derived from Secondary Reprogramming

(A) SNP analysis of allelic-specific expression of X-linked *GRPR* gene in iPSC (D551-iPSCK1) derived from Detroit 551 fibroblasts, differentiated fibroblasts (dfD551-K1), and secondary iPSC clones from dfD551-K1. When monoallelic dfD551-K1 cells having TT SNP in *GRPR* were reprogrammed, secondary iPSC clones that express TT SNP (dfD551K1-iPSC32), AA SNP (dfD551K1-iPSC22), or TT/AA (dfD551K1-iPSC21) were generated.

(B) RNA FISH for *XIST* in secondary iPSC lines at passage 12. Monoallelic dfD551-PSC32 shows XIST clouds, whereas biallelic dfD551K1-iPSC21 does not, confirming the X chromosome status. Scale bar, 20 μm.

(C) Immunostaining of H3K27me3 and OCT4 in secondary iPSC lines derived from dfD551-K1 fibroblasts. dfD551K1-iPSC32 shows H3K27me3 foci, representing the presence of inactive X chromosome, whereas dfD551K1-iPSC21 does not. Nuclei were counterstained with DAPI. Scale bar, 20 μm.

(D) Immunostaining of H3K27me3 (red) in Detroit 551 fibroblasts undergoing reprogramming on the indicated days. GFP (green) represents the expression of retrovirus-mediated reprogramming factors, and nuclei were counterstained with DAPI (blue). GFP+ cells under reprogramming lose H3K27me3 foci. Scale bar, 20 μm.

(E) Quantification of the H3K27me3 foci+ and H3K27me3 foci− cells in (A). Error bars represent mean ± SEM of three independent experiments.

(F) Relative expression of total (upper panel) and ectopic (lower panel) *OCT4*, *SOX2*, *KLF4*, and *MYC*.

(G) Relative mRNA expression of genes involved in XCI and pluripotency during reprogramming. Homogeneous populations of Detroit 551 fibroblasts undergoing reprogramming were sorted according to the expression of fibroblast marker CD13, pluripotency markers SSEA4 and TRA160, and retroviral GFP. Error bars represent mean ± SEM of three independent experiments.

spreading on the X chromosome is essential for XCI. Recently, the LIM-domain protein RNF12 was shown to be a positive transcription activator for *XIST* (Gontan et al., 2012; Navarro et al., 2011). The expression of *XIST* and *RNF12* decreased during reprogramming, consistent with the decrease in the percentage of cells with H3K27me3-positive foci, whereas the pluripotency markers increased (Figure S2D). Previously, we found that reprogramming is a progressive process that can be defined by the change in cell-surface markers and the retroviral gene expression (Chan et al., 2009). Prior to reprogramming, fibroblasts express the cell-surface marker CD13, which is rapidly repressed by the expression of reprogramming factors marked by the expression of GFP contained in retroviral vector. The silencing of GFP marks the formation of bona fide iPSCs that express SSEA4 and TRA160 cell-surface markers (Chan et al., 2009). These cell-surface markers can be utilized to further dissect and isolate cells in progressive reprogramming stages: CD13+GFP-SSEA4-TRA160−, fibroblasts; CD13-GFP+SSEA4+TRA160−, partially reprogrammed cells; and CD13-GFP-SSEA4+TRA160+, fully reprogrammed cells (Chan et al., 2009). Using fluorescence-activated cell sorting (FACS), we isolated cells using a combination of markers and purified total RNA, and performed a gene-expression analysis (Figure 1F). CD13+ fibroblasts that had strong H3K27me3 foci showed high expression of *XIST* and *RNF12*, which is consistent with their role in XCI. CD13-GFP+ cells that were isolated at days 14 and 28 after reprogramming showed high expression of ectopic reprogramming factors and a dramatic reduction in expression of *XIST* and *RNF12* (Figures 1F and 1G). When cells became bona fide iPSCs and expressed TRA160, the ectopic expression of four reprogramming factors was dramatically reduced (Figure 1F). These data suggest that the high expression of ectopic reprogramming factors induces X reactivation during reprogramming.

In order to rule out the possibility that the presence of contaminating cells with the opposite SNP of genes in parental fibroblasts is responsible for the formation of secondary iPSC clones with the opposite SNP, we used female fibroblasts from Lesch-Nyhan syndrome (LNS) cells with a mutation in *HPRT*. LNS fibroblasts display a mosaic pattern of X-linked *HPRT* expression. Fibroblasts that have mutant *HPRT* on an active X chromosome ($Xa^{HPRT-}Xi^{HPRT+}$), and therefore lack HPRT activity, are sensitive to hypoxanthine-aminopterin-thymidine (HAT) in medium. However, they do not metabolize 6-thio-guanine (6TG), whose toxic metabolites kill cells with an active HPRT, and thus they can grow in medium with 6TG. In contrast, fibroblasts with a wild-type *HPRT* allele on an active X chromosome ($Xa^{HPRT+}Xi^{HPRT-}$) are resistant to HAT but sensitive to 6TG (Figure 2A). Using this differential sensitivity to HAT and 6TG, we isolated two homogeneous cell populations: one with 6TG resistance (fLNS-6TG [$Xa^{HPRT-}Xi^{HPRT+}$]) and one with HAT resistance (fLNS-HAT [$Xa^{HPRT+}Xi^{HPRT-}$]). In order to test the stability of drug selectivity, cells that were selected with either drug were cultured without the drug for 2 weeks, and then drug sensitivity was tested. fLNS-HAT fibroblasts previously selected for HAT resistance showed no resistance to 6TG, and fLNS-6TG fibroblasts previously selected for 6TG did not survive in the HAT condition (Figure S3A). These data suggest that XCI states in the drug-selected cells were stably maintained. These two homogeneous populations of cell lines having only one active X chromosome were reprogrammed. We examined the X chromosome status of iPSC clones by testing the drug sensitivity and analyzing SNPs of genes on the X chromosome (Figure 2A). Like the iPSCs derived from clonally differentiated dfD551-K1, the iPSC clones that were generated from fLNS-6TG had different X chromosome states and drug sensitivities: 6TG-iPSC3, 6TG resistance ($Xa^{HPRT-}Xi^{HPRT+}$); 6TG-iPSC1, HAT resistance ($Xa^{HPRT+}Xi^{HPRT-}$); and 6TG-iPSC6, HAT resistance ($Xa^{HPRT+}Xa^{HPRT-}$; Figure 2B). In addition to drug resistance, we performed a SNP analysis in the X-linked *GYG2* gene. Consistent with drug-resistance phenotypes, these iPSC clones showed allelic specificity (at nucleotide 1,127 of mRNA) of the *GYG2* gene: 6TG-iPSC3, (G) SNP; 6TG-iPSC1, (A) SNP; and 6TG-iPSC6, (G/A) SNPs (Figure 2B). The generation of HAT-resistant clones (e.g., 6TG-iPSC1) from 6TG-selected fibroblasts further supports our finding that XCR occurs during reprogramming. In order to further confirm the conversion of the drug sensitivity of iPSCs, we differentiated 6TG-resistant monoallelic 6TG-iPSC3 and generated df6TG-3 fibroblast ($Xa^{HPRT-}Xi^{HPRT+}$). df6TG-3 cells were reprogrammed (Figure 2A). HPRT activity and SNP were again examined with secondary iPSC clones. As with the iPSC clones derived from drug-selected primary fibroblasts, the converted SNP and HPRT activities were observed in secondary iPSC lines (Figure 2C). When six secondary iPSC clones from df6TG-3 were treated with either 6TG or HAT, two clones showed resistance only to 6TG. The other four clones died under the 6TG culture condition, but survived in the presence of HAT in the medium (Figure 2C). In addition, SNP of the X-linked *GYG2* gene was examined. Two of six df6TG3-iPSC clones had the same SNP (at 998 nt of mRNA) *GYG2* (T) as the parental df6TG-3 cells ($Xa^{HPRT-}Xi^{HPRT+}$). Out of four df6TG3-iPSC clones that acquired HAT resistance, two showed monoallelic (C) SNP in *GYG2* ($Xa^{HPRT+}Xi^{HPRT-}$), and the other two showed biallelic SNP patterns ($Xa^{HPRT-}Xa^{HPRT+}$; Figure S3B). The differential *GYG2* SNPs were also confirmed via restriction-enzyme-sensitive digest (Figure 2D). *GYG2* SNPs (either C or T) were differentially cleaved depending on the XCI status, as shown in Figure 2D, and strongly correlated with the status of H3K27me3 foci (Figure 2E).

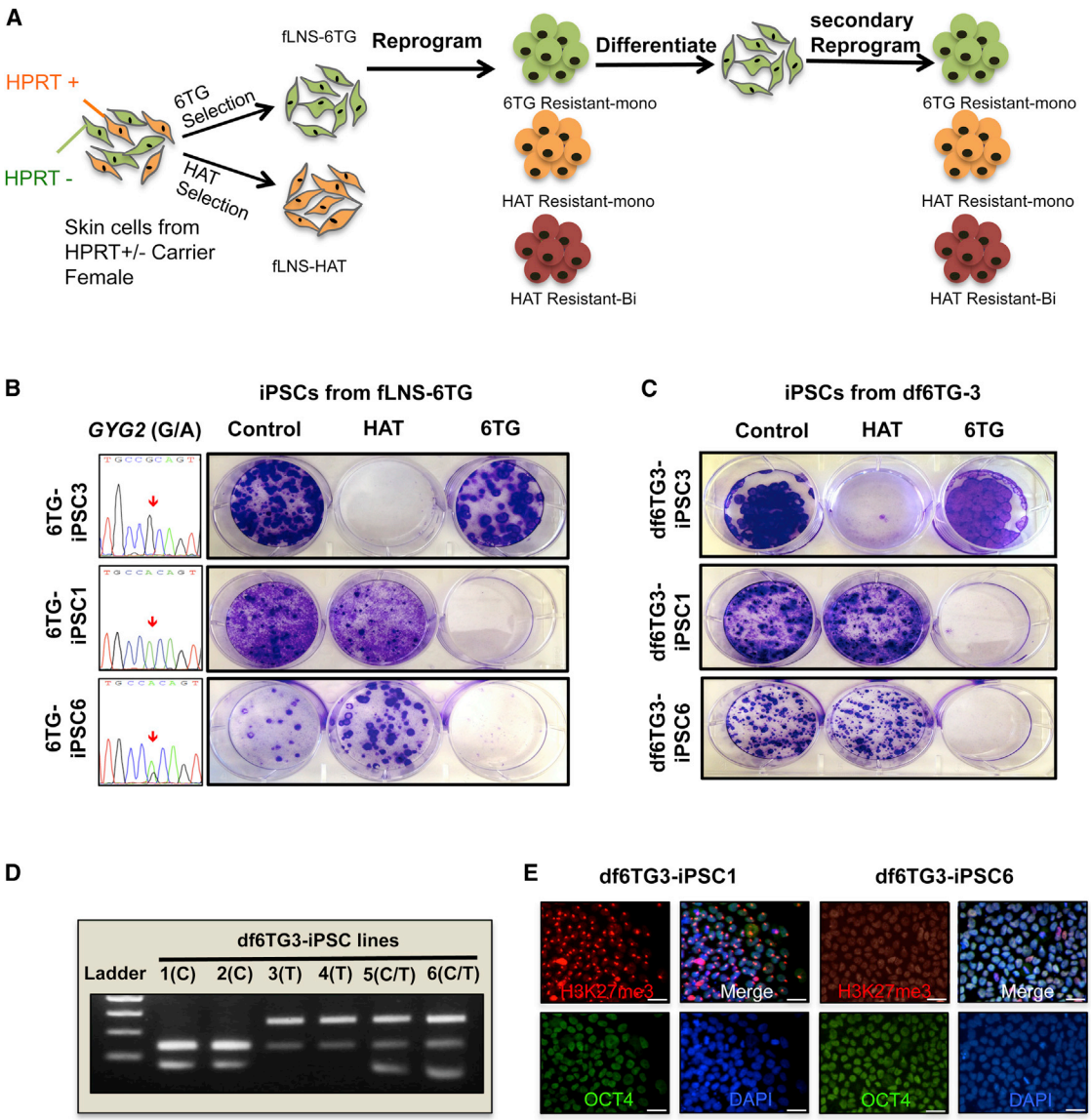

Figure 2. Formation of Female iPSCs with a Different X Chromosome State Compared with the Parental fLNS-6TG ($Xa^{HPRT-}Xi^{HPRT+}$) Fibroblast

(A) Schematic representation of strategy for generating homogeneous fibroblasts from LNS patients with a *HPRT* mutation. Culture with 6TG or HAT produces two homogeneous populations of fibroblasts with X chromosome in either the ($Xa^{HPRT-}Xi^{HPRT+}$, fLNS-6TG) or ($Xa^{HPRT+}Xi^{HPRT-}$, fLNS-HAT) state.

(B) Generation of HAT-resistant clones from 6TG-selected fLNS-6TG fibroblasts. Allelic-specific expression of *GYG2* is shown in the left column, and resistance to HAT or 6TG is shown by crystal violet staining of iPSC clones after treatment with HAT or 6TG for 10 days.

(C) Generation of HAT-resistant secondary iPSC clones from 6TG-resistant fibroblasts (df6TG-3) of the 6TG-resistant iPSC clone (6TG-iPSC3). Crystal violet staining of secondary iPSC lines after selection with HAT or 6TG is shown.

(D) Analysis of allele-specific expression of *GYG2* in secondary iPSC lines via restriction-enzyme-sensitive SNP. Allele-specific *GYG2* SNPs were amplified by PCR and digested with BstIMutI restriction enzyme.

(E) Representative images of H3K27me3/OCT4 immunostaining with secondary df6TG-iPSC lines. Scale bar, 20 μm.

A similar conversion of X chromosome status or the reactivation of the inactive X chromosome was found in reprogramming fLNS-HAT (Xa^{HPRT+} Xi^{HPRT-}) and secondary reprogramming dfHAT-1 (Xa^{HPRT+} Xi^{HPRT-}). Not only HAT-resistant iPSCs but also 6TG-resistant iPSC clones were isolated from reprogramming of fLNS-HAT cells and dfHAT-1 cells (Figure S3C). The allelic specificity of the X chromosome of dfHAT1-iPSC was further supported by

SNP analysis of *MAOA* and *GYG2*, and H3K27me3 staining (Figures 2E and S3D–S3F). These results support our finding that reactivation of the inactive parental X chromosome occurs, followed by inactivation.

Reprogramming Activates the Inactive X Chromosome in Female Fibroblasts

We reasoned that if XCR occurs, cells with converted drug resistance might arise from cells undergoing active reprogramming. In order to test this hypothesis, we induced the reprogramming of fLNS-6TG cells (Xa^{HPRT-} Xi^{HPRT+}) and tested the 6TG and HAT resistance during reprogramming. At 10 days after reprogramming, we added HAT or 6TG into the reprogramming medium and continued reprogramming for an additional 2 weeks. Remarkably, iPSC colonies that were resistant to HAT arose (Figure 3A), suggesting that a reactivation of the inactive X chromosome occurs during reprogramming. Previous studies (Mekhoubad et al., 2012; Tchieu et al., 2010) reported that the X chromosome status is maintained during reprogramming. The Plath group used a lentiviral vector system that expresses four reprogramming factors in one backbone (STEMCCA vector), whereas we used a retroviral vector, which may explain the difference in results. Thus, we tried to reprogram the fLNS-6TG with STEMCCA vector. However, we could isolate iPSC colonies with an opposite X chromosome state (HAT-resistant clones; Figure 3A). Thus, the reprogramming vectors do not seem to be responsible for the reactivation of the X chromosome. The relatively high expression of reprogramming factors in our reprogramming condition may have resulted in reactivation of the X chromosome during reprogramming. We performed Southern blot analysis in 12 iPSC clones that were characterized for their X chromosome status (Figure S3G). No clones showed the same provirus integration patterns. A total of >30 provirus integrations and eight integrations of OCT4 or SOX2 were found in each clone (Figure S3G). No previous studies have directly addressed the relationship between the X chromosome status of female iPSCs and the total number of provirus integrations. However, the female iPSC clones derived from three independent individuals via the reprogramming protocol of the Eggan group showed two to six integrations in OCT4 provirus and two to four integrations in SOX2 provirus (see Figure S6 in Boulting et al., 2011), which is fewer than observed in the iPSC clones generated in our protocol. Thus, the reactivation of the inactive X chromosome in iPSC clones in our protocol may be due to the higher expression of the four factors during reprogramming. Since human ESCs with two active X chromosomes were successfully derived under the hypoxic condition, we tested whether the hypoxic reprogramming condition prevents the formation of an inactive X chromosome (Lengner et al., 2010). As in the normoxic condition, we obtained iPSC colonies from fLNS-6TG that showed HAT resistance as well as 6TG resistance (Figure 3A). The production of 6TG-resistant clones with only one active X chromosome suggests that hypoxic reprogramming conditions do not maintain the two active X chromosomes, consistent with a previous report (Pomp et al., 2011). We then asked whether the HAT resistance acquired by fLNS-6TG during the reprogramming accompanied the reactivation of XCI. At 14 days of reprogramming, the *GYG2* and *MAOA* SNPs showed a biallelic pattern: *GYG2* (C and T at 998 nt), *GYG2* (A and G at 1,127 nt), and *MAOA* (A and G) (Figure 3B). Overall, our data showed that reprogramming reactivates the inactive X chromosome of fibroblasts.

We also took advantage of a monoallelic RTT3-iPSC-46m clone isolated from RTT3 fibroblasts to analyze the transcriptional activation of inactive X chromosome during reprogramming (Kim et al., 2011). RTT3 fibroblasts originate from a female RTT patient who had a nucleotide deletion (705 delG) in the middle of *MECP2*. This deletion causes a frameshift in the codon and ultimately produces C-terminal deletion MECP2 protein. The RTT3-iPSC-46m clone is monoallelic and expresses only mutant *MECP2* allele (Figure 3F). Thus, the antibody against the C terminus of MECP2 does not recognize it. We differentiated RTT3-iPSC-46m iPSCs into fibroblasts to produce dfRTT3-46m cells. The inactive X chromosome status was maintained in dfRTT3-46m, and an antibody for C-terminal MECP2 did not detect mutant MECP2. We initiated reprogramming of dfRTT3-46m and analyzed the production of MECP2 at days 14 and 21 by performing western blotting and immunostaining. Remarkably, we found that cells undergoing reprogramming produced wild-type MECP2 from days 14 and 21 (Figures 3C–3E). These results provide definitive evidence that the XCR that resulted in loss of H3K27m3 foci and low expression of *XIST* and *RNF12* upon reprogramming had become a state in which transcription was active.

Nascent iPSCs Contain the Inactivated X Chromosome

If the inactive X chromosome becomes activated during reprogramming, how are the monoallelic iPSCs that have one active X chromosome produced? In order to answer this question, we performed an extensive analysis of change in the X chromosome state in established iPSC clones. Our previous analysis of cellular marks during programming found that the silencing of retrovirus-mediated GFP expression occurs when cells become fully reprogrammed and make faithful iPSCs (Chan et al., 2009; Kim et al., 2012). At 28 days after reprogramming, when iPSC colonies arose, we examined X chromosome status by staining cells for H3K27me3. Unexpectedly, we found that all of the nascent iPSC colonies with no GFP expression displayed H3K27me3 foci, suggesting that all of them had an inactive X chromosome (Figure 4A). In order

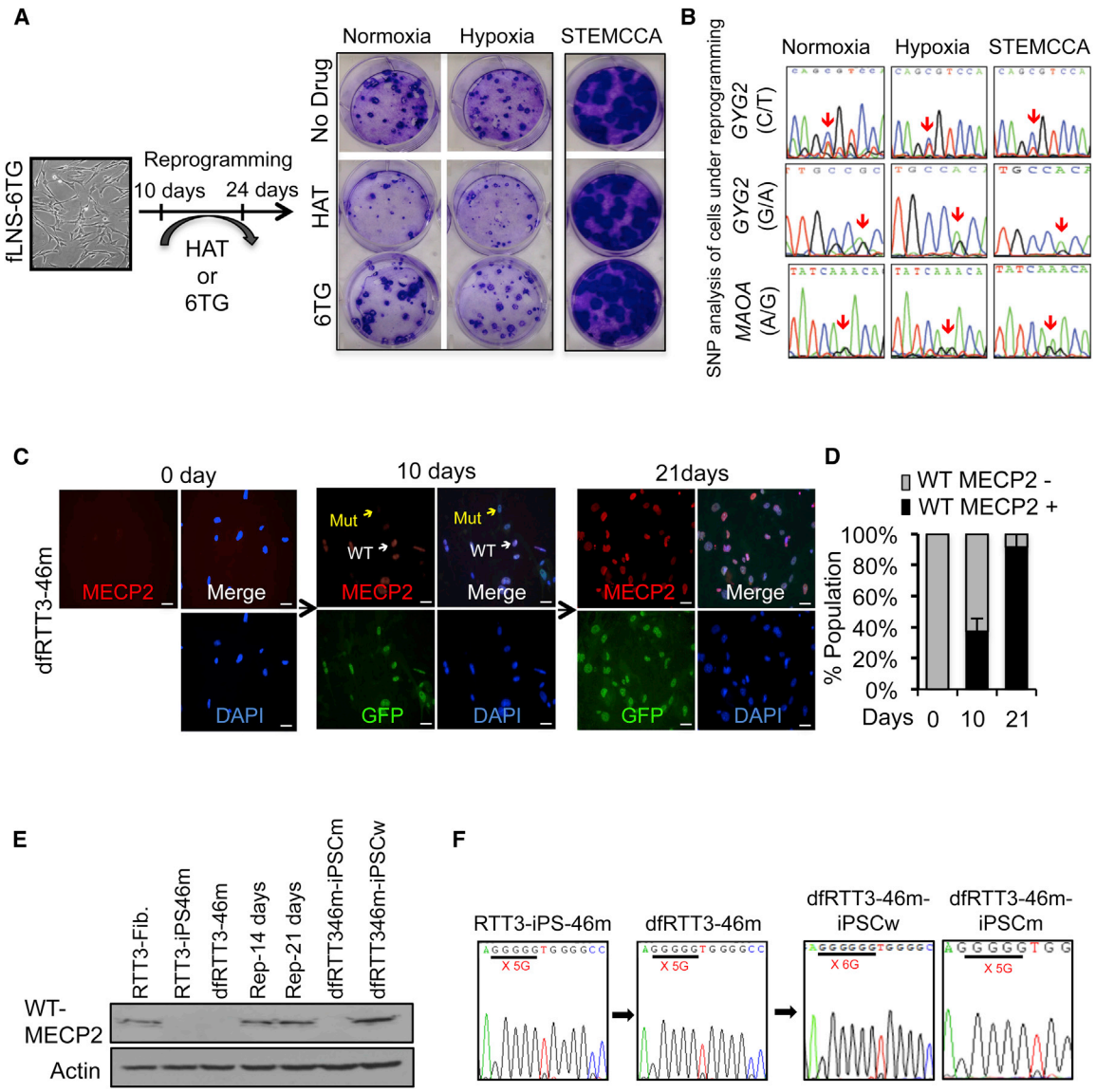

Figure 3. XCR during Active Reprogramming

(A) Crystal violet staining of a reprogrammed whole cell in a six-well plate. 6TG-resistant fLNS-6TG ($Xa^{HPRT-}Xi^{HPRT+}$) cells were induced for reprogramming in a normoxic or hypoxic condition using pMIG retroviral vector, or in a normoxic condition using STEMCCA lentiviral vector. After 10 days, reprogramming was continued in medium with HAT or 6TG for 2 weeks. Seven days after HAT was withdrawn, the plate was stained for crystal violet. In all three conditions, iPSCs with resistance to HAT were formed.

(B) Allelic-specific sequencing of *GYG2* and *MAOA* in cells under 14 days of reprogramming.

(C) Immunostaining of wild-type (WT) MECP2 in dfRTT3-46m cells undergoing reprogramming at the indicated times with antibody recognizing the C terminus of MECP2 (red) and DAPI (blue). White arrows indicate WT of MECP2 and yellow arrows indicate the mutant type of MECP2. Scale bar, 20 μm.

(D) Quantification of WT MECP2+ cells in dfRTT3-46m cells undergoing reprogramming in (C). Four randomly chosen fields were used to count the number of MECP2+ cells and to calculate the percentage. Error bars represent mean ± SEM.

(E) Protein expression of WT of MECP2 in dfRTT3-46m fibroblasts undergoing reprogramming. At 10 and 21 days after reprogramming, whole-cell extracts were immunoblotted for MECP2 antibody recognizing the C terminus of MECP2.

(F) Representative SNP of *MECP2* in secondary iPSCs.

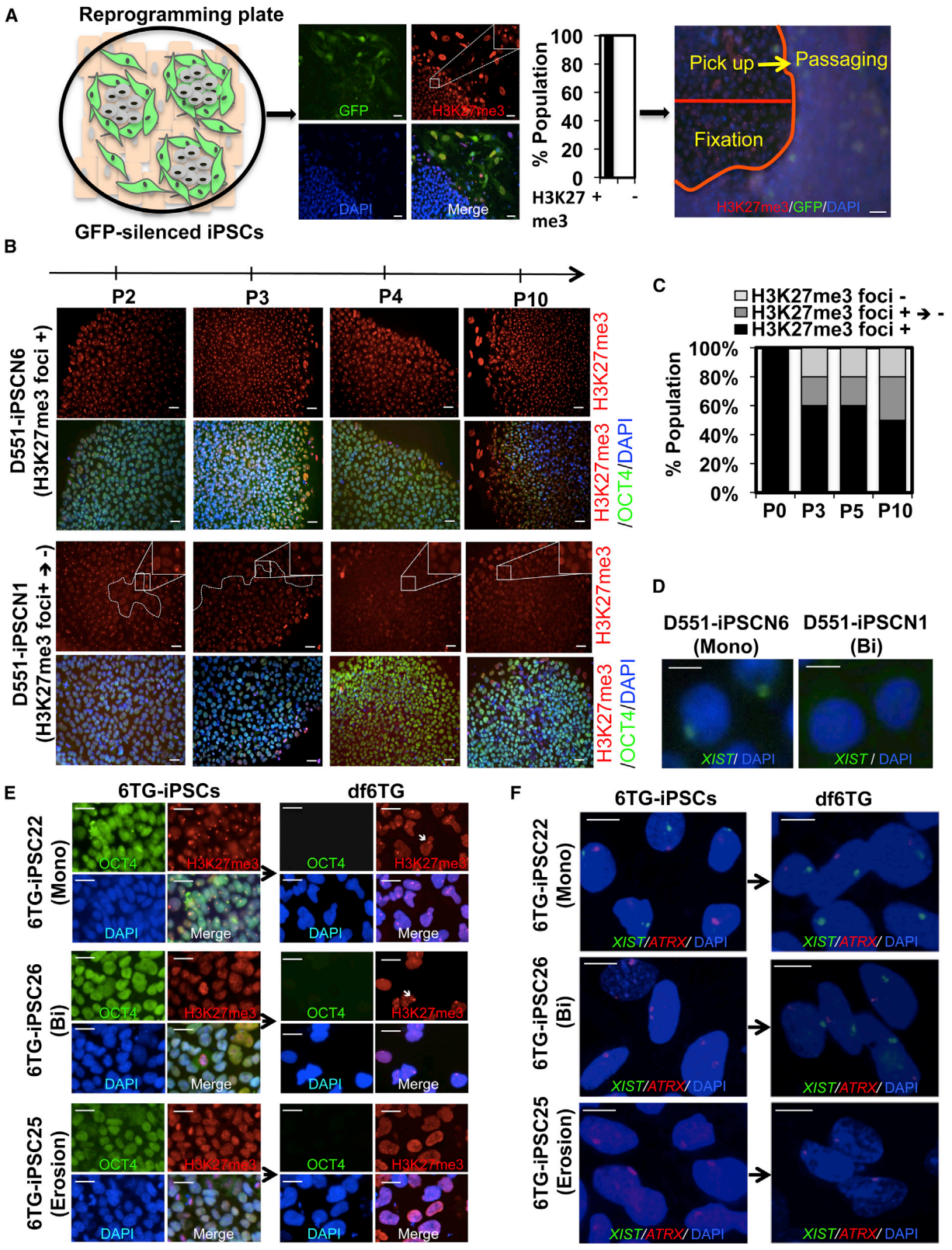

(legend on next page)

to examine the *XIST* and *RNF12* expression in GFP− colonies, we performed quantitative PCR in cells isolated using surface markers and GFP expression. Consistent with the change in H3K27me3 staining, the expression of *XIST* and *RNF12* together with pluripotency markers was highly upregulated in the SSEA4+/TRA160+/GFP− population isolated at day 28, whereas cells that showed GFP and thus had high expression of reprogramming factors showed low expression of *RNF12* and *XIST* (Figures 1G and S2E). Thus, it seems that before cells become fully reprogrammed, the X chromosome is in an active state, perhaps due to the suppression of *XIST* and *RNF12*. The silencing of ectopic reprogramming factors activates *XIST* and *RNF12*, and the X chromosome becomes inactivated and marked by precipitous H3K27me3 foci formation in nascent iPSC clones (Shin et al., 2010). These results suggest that the active X chromosome during reprogramming is transient and the X chromosome becomes inactivated following completion of reprogramming, leading to the formation of a monoallelic X chromosome state in newly formed nascent iPSC clones.

XCR in iPSCs

Although the initial female iPSC colonies displayed the marker for an inactive X chromosome in the current study (Figure 4A), other groups and we have previously reported the isolation of biallelic iPSCs with two active X chromosomes from female somatic cell reprogramming (Kim et al., 2011; Marchetto et al., 2010; Tomoda et al., 2012). It seems that biallelic iPSCs arise during picking and expansion. In order to test this, we closely examined X chromosome status in iPSC clones at each passage after the initial picking. First, the nascent iPSC clones picked from the original reprograming plate were denoted as "passage 0." We picked ten iPSC colonies without GFP expression from a plate of reprogrammed Detroit 551 or RTT3 fibroblasts. During passaging, half of the colonies were picked up for the next passage and the other half were fixed for H3K27me3 staining (Figures 4A and S4A). We repeated the picking and passaging up to passage 10. At each passage, we examined the H3K27me3 status in iPSC colonies. Interestingly, four out of ten D551-iPSC colonies started to show an area without H3K27me3 foci following passage 1 or 2 (Figures 4B, 4C, and S4B). All cells in the clones that had begun to lose H3K27me3 foci eventually became H3K27me3 foci- and *XIST*-negative. The remaining six colonies maintained the H3K27me3 and *XIST* foci (Figures 4B–4D, S4C, and S4D). This gradual gaining of H3K27me3 foci-negative cells and the loss of *XIST* expression were also observed in iPSC clones from fLNS-HAT and fLNS-6TG fibroblasts (Figures S4E and S4F). These data suggest that either monoallelic iPSCs become biallelic iPSCs after picking and expansion or a few biallelic iPSCs exist in the colonies that have a growth advantage, and they become dominant cells during picking and expansion. Our current data cannot exclude either possibility.

The absence of H3K27me3 foci and *XIST* expression in iPSCs suggests that these cells are class I iPSCs that have two active X chromosomes. However, the continuous culture of class II iPSCs can result in a partial reactivation of the inactive X chromosome due to an epigenetic change of the X chromosome (so-called "erosion"), resulting in class III iPSCs (Mekhoubad et al., 2012). Erosion and full reactivation can be distinguished by the formation of H3K27me3 foci and *XIST* expression in cells differentiated from iPSCs. In order to determine whether iPSC clones that have no H3K27me3 foci or *XIST* are class I or class III iPSCs, we differentiated 12 iPSC clones derived from fLNS-6TG fibroblasts by treating them with retinoic acid for 14 days. The formation of H3K27me3 foci, *XIST*, and *ATRX* cloud

Figure 4. Formation of Class I and Class III iPSC Clones in Early Passaging

(A) Schematic of tracing the X chromosome after reprogramming. iPSCs undergo rapid XCI upon completion of reprogramming, and all GFP-silenced nascent iPSC colonies display H3K27me3 foci. In order to trace the X chromosome status after reprogramming, half of the colonies were fixed and half were used for passaging. Scale bar, 20 μm.

(B) Appearance of H3K27me3 foci-negative cells in iPSC clones during passaging. H3K27me3 foci-positive D551-iPSCN1 iPSCs became H3K27me3 foci-negative cells upon passaging, whereas D551-iPSCN6 remained an H3K27me3 foci-positive clone. Scale bar, 20 μm.

(C) Percentage of iPSC clones that underwent the H3K27me3 foci-positive to -negative transition during passaging in (B). A total of ten H3K27me3 foci-positive Detroit 551-derived iPSC clones were picked and expanded to trace the change of H3K27me3 status.

(D) FISH for *XIST* RNA in iPSCs at passage 10 to determine the X chromosome status. Scale bar, 20 μm.

(E) Representative images of H3K27me3 and OCT4 staining in 6TG-iPSCs at passage 10 and differentiated cells. 6TG-iPSC22 is a class II iPSC and displays H3K27me3 foci before and after differentiation. 6TG-iPSC26 is a class I iPSC and shows formation of H3K27me3 foci only after differentiation. 6TG-iPSC25 is a class III iPSC, and no H3K37me3 foci exist before or after differentiation. Arrow indicates H3K27me3 foci. Scale bar, 20 μm.

(F) Representative images of *XIST* and *ATRX* FISH in 6TG-iPSCs at passage 10 and differentiated cells. 6TG-iPSC22 is a class II iPSC and displays one *XIST* and one *ATRX* focus before and after differentiation. 6TG-iPSC26 is a class I iPSC and shows formation of *XIST* after differentiation. Two *ATRX* foci become one after differentiation. 6TG-iPSC25 is a class III iPSC, and no *XIST* foci exist before or after differentiation. Scale bar, 20 μm.

was examined by fluorescence in situ hybridization (FISH). Six of 12 clones showed an X chromosome status of class II type, having *XIST* and H3K27me3 foci in iPSCs and differentiated cells (e.g., 6TG-iPSC22; Figures 4E and 4F). The other six iPSC clones showed no H3K27me3 foci or *XIST* cloud before differentiation, suggesting that they were either class I or class III iPSC clones. In three clones, H3K27me3 foci and *XIST* cloud arose after differentiation, confirming that they were class I iPSC clones (e.g., 6TG-iPSC26; Figures 4E and 4F). Meanwhile, the other three clones did not show H3K27me3 foci or *XIST* cloud after differentiation, representing the "eroded" state of the X chromosome (6TG-iPSC25; Figure 4F). SNPs in *GYG* and *MAOA* genes of 12 iPSCs further confirmed the allelic expression of X chromosome genes (Table 1). Our results indicate that either class I or class III iPSCs can arise from nascent iPSC colonies with inactive X chromosome marks.

DISCUSSION

Here, we demonstrate that the status of the X chromosome is dynamic during human female somatic cell reprogramming. Extending previous studies that examined X chromosome status in iPSCs after completion of reprogramming, we determined the change of X chromosome status in cells at different stages of reprogramming and after they were established as iPSC clones. We found that strong ectopic expression of reprogramming factors markedly suppresses *XIST* and RNF12, and mediates the reactivation of the inactive X chromosome (reprogramming XCR [rXCR] in Figures S5D). Although it is transient, the reactivated X chromosome at rXCR is transcriptionally active (Figure 3). When reprogramming was completed, the nascent iPSC clones were shown to be composed mostly of cells possessing the inactive X chromosome marker H3K27me3 foci. These results suggest that the reactivated X chromosome state in cells under active reprogramming is transient, and the timing of inactivation of the X chromosome is well correlated with the silencing of ectopic reprogramming factors (Chan et al., 2009). In murine ESCs, the reprogramming factors Oct4 and Nanog bind to intron 1 of *Xist* and suppress its transcription, whereas Myc and Klf4 bind to *DXPas34* of *Tsix* to activate the transcription, resulting in two active X chromosomes (Deuve and Avner, 2011). Likewise, the high expression of the reprogramming cocktail in the current study may suppress *XIST* in cells undergoing reprogramming and reactivate the inactive X chromosome. When cells become bona fide iPSCs, the retroviral silencing machinery becomes activated (Chan et al., 2009; Matsui et al., 2010) and reduces the ectopic expression of reprogramming factors and thus the suppression of *XIST*. Remarkably, the formation of monoallelic iPSC clones composed of the same inactive X chromosome indicates that out of many cells undergoing reprogramming, only one cell becomes an iPSC clone and thus has one allele of the inactive X chromosome.

Tracing of the nascent iPSC clones that were composed mostly of H3K27me3 foci-positive cells showed that cells with no H3K27me3 markers became dominant in some clones during very early passages. There are two possible explanations for this: either H3K27me3 foci-positive class II iPSCs become H3K27me3 foci-negative class I or class III cells, or some existing H3K27me3 foci-negative iPSCs that have a growth advantage become dominant during passaging. In a detailed analysis of the X chromosome state, we found that class I iPSCs with two active X chromosomes, as well as class III iPSCs with one active and one eroded X chromosome, arose in early passages (Figure 4F). Although a previous report by the Eggan lab suggested that the long-term culture of iPSCs results in X chromosome erosion (Mekhoubad et al., 2012), our data show that X chromosome erosion occurs even in very early passages. Currently, it is unknown how class I iPSC clones arise from class II nascent iPSCs. Perhaps the neighboring non-reprogrammed cells suppress the XCR in nascent iPSCs via paracrine factors (Bendall et al., 2007; Xu et al., 2005), and when the iPSCs are picked and placed in a new culture plate without the influence of these factors, XCR may occur. During development, the X chromosome shows dynamic changes in state. The X chromosome becomes activated in the ICM in mouse (Lessing et al., 2013). Preimplantation human embryos also show two X chromosomes in the pre-XCI state (Lengner et al., 2010; Okamoto et al., 2011). Following random inactivation in the epiblast stage, the X chromosome becomes reactivated in PGC development (Sugimoto and Abe, 2007). The reactivation of the X chromosome during reprogramming shown by our results suggests that reprogramming mimics either preimplantation embryo development or PGC formation where XCR occurs.

iPSC clones with different X chromosome status have been isolated by several groups (Ananiev et al., 2011; Cheung et al., 2011; Pomp et al., 2011; Tchieu et al., 2010). Some groups isolated iPSCs with one active X chromosome and others isolated two active X chromosomes. The medium used for reprogramming does not seem to be responsible for the different results, because all of these groups used a standard medium composed of knockout serum replacement and basic fibroblast growth factor (Amit et al., 2000). The reprogramming methods used by each group may not result in iPSCs with different X chromosome status. The Plath group used retro- or lentiviral polycistronic vectors that express four reprogramming factors in one backbone (Tchieu et al., 2010). The Ellis, Colman, Chang, and Eggan groups all used retrovirus for

reprogramming (Ananiev et al., 2011; Mekhoubad et al., 2012; Pomp et al., 2011). We used a lentiviral STEMCCA vector that was used by the Plath group (Figure 3A). Although the Plath group did not report XCR, we found that the STEMCCA vector gives rise to iPSCs with XCR. Thus, the vectors used for reprogramming do not unambiguously explain the differential X chromosome status in iPSCs. Although isogenic iPSC clones can be isolated from reprogramming of female fibroblasts, some of the above-cited papers reported that monoallelic iPSC clones with only one inactive X chromosome, but no other X chromosomes, were isolated from some lines (Cheung et al., 2011; Pomp et al., 2011), whereas we readily isolated iPSC clones with two different X chromosome states. OCT4, SOX2, MYC, and KLF4 were shown to play critical roles in reactivation of the inactive X chromosome (Deuve and Avner, 2011; Lessing et al., 2013; Navarro et al., 2010). Differences in viral infectivity or the amount of virus added may have influenced the expression of reprogramming factors and thus X chromosome state during reprogramming. Indeed, the analysis of provirus integration in our iPSC clones showed many more integrations compared with those derived by the Eggan group (Figure S3G; Boulting et al., 2011; Mekhoubad et al., 2012). Another possibility is the difference in the fibroblast line of resistance to reprogramming, for which the epigenetic barriers may prevent the XCR during reprogramming. The different feeder conditions used cannot be ruled out as a possible cause, since the Yamanaka group showed that feeder cells that produce high LIF support the derivation of iPSCs with two active X chromosomes (Tomoda et al., 2012). However, the feeder we used does not express high LIF and is less likely to be a cause of X reactivation.

Considering the importance of female iPSCs for disease modeling and future cellular therapeutics, it is critical to acquire concrete information about the X chromosome state in given iPSC clones. X-linked monogenic diseases show different penetrance in males and females depending on the recessive or dominant role of the mutated genes (Dobyns et al., 2004). Maintaining one of the inactive X chromosomes in an inactive state in female iPSCs will be essential, especially for studying diseases such as Duchenne muscular dystrophy, hemophilia A and B, and α-thalassemia, where there is a low penetrance in the female and the mutated genes are recessive (Dobyns et al., 2004). When applying the in vitro differentiated derivatives of female iPSCs as therapeutics, it will be crucial to maintain the XCI because epigenetically unstable *XIST*-negative cells express oncogenes (Anguera et al., 2012) and could lead to tumor, as reported in *XIST*-depleted leukemia in a murine model (Yildirim et al., 2013). Thus, our current study delineating the X chromosome status of cells during and after reprogramming provides an important foundation for the use of female iPSCs in disease modeling and cell therapeutics.

EXPERIMENTAL PROCEDURES

Cell Culture and Reprogramming

Normal primary fibroblasts Detroit 551, WI38, and IMR90 were purchased from the American Type Culture Collection (CCL-110, CCL-75, and CCL-186, respectively). Fibroblast cell lines from patients with RTT (RTT3, GM07982; RTT4, GM11270; and RTT5, GM17567) and fLNS-HPRT$^{+/-}$ (GM02226) were obtained from the Coriell Institute for Medical Research. iPSCs were reprogrammed and maintained as described in Supplemental Experimental Procedures. dfD551-K1, dfRTT1-13w, dfRTT3-46m, dfRTT4-24w, and dfRTT5-34m were generated by differentiating monoallelic D551-iPSCK1, RTT1-iPSC-13w, RTT3-iPSC-46m, RTT4-iPSC-24w, and RTT5-iPSC-34m iPSC lines, respectively, into fibroblast-like cells. To induce differentiation, iPSCs were dissociated using Accutase (Millipore) with the addition of rock inhibitor (Y27632; Sigma), and cells were plated on gelatin-coated plates. Cells were cultured in Dulbecco's modified Eagle's medium with 15% fetal bovine serum and nonessential amino acid over 4 weeks, and used for reprogramming.

HAT and 6TG Selections

In order to isolate two homogeneous subpopulations of fLNS-HAT ($Xa^{HPRT+}Xi^{HPRT-}$) and fLNS-6TG ($Xa^{HPRT-}Xi^{HPRT+}$) from HPRT$^{+/-}$ fibroblasts, cells were incubated with culture medium containing either 60 μM of 6TG or 1× HAT for 14 days. Each selected subpopulation was used for reprogramming to generate iPSCs. In order to determine the allelic specificity of *HPRT* in iPSC clones derived from fLNS-HAT and fLNS-6TG subpopulations, iPSCs were treated with collagenase and plated as small colony clumps in six-well plates coated with mouse embryonic fibroblasts. Three days after plating, cells were cultured with human ESC culture medium containing HAT or 6TG for 10 days. Cells were fixed with 4% formaldehyde/PBS and stained with crystal violet.

Gene-Expression and SNP Analyses

RNA was isolated from iPSCs using an RNeasy minikit (QIAGEN), and 1 μg of RNA was used for reverse transcription with iScript (BioRad) according to the manufacturer's protocol. Gene-expression and SNP analyses were performed as described in Supplemental Experimental Procedures.

Immunostaining

iPSCs or cells undergoing reprogramming were fixed for 10 min at room temperature with 4% paraformaldehyde in PBS and stained as described in Supplemental Experimental Procedures.

FISH for XIST/ATRX, Western Blot, and Southern Blot

RNA FISH was carried out as described previously (Tchieu et al., 2010). Detailed methods for FISH, western blot, and Southern blot are described in Supplemental Experimental Procedures.

SUPPLEMENTAL INFORMATION

Supplemental Information includes Supplemental Experimental Procedures, five figures, and two tables and can be found with this article online at http://dx.doi.org/10.1016/j.stemcr.2014.04.003.

ACKNOWLEDGMENTS

We thank Dr. Andrew Xiao for use of Olympus IX81 and radioisotope protective equipment. I.-H.P. was partly supported by the NIH (GM0099130-01); the CSCRF (12-SCB-YALE-11); the KRIBB/KRCF Research Initiative Program (NAP-09-3); CTSA grant UL1 RR025750 from the National Center for Advancing Translational Science (NCATS), a component of the NIH; and the NIH Roadmap for Medical Research.

Received: July 11, 2013
Revised: April 5, 2014
Accepted: April 7, 2014
Published: May 15, 2014

REFERENCES

Abyzov, A., Mariani, J., Palejev, D., Zhang, Y., Haney, M.S., Tomasini, L., Ferrandino, A.F., Rosenberg Belmaker, L.A., Szekely, A., Wilson, M., et al. (2012). Somatic copy number mosaicism in human skin revealed by induced pluripotent stem cells. Nature *492*, 438–442.

Amit, M., Carpenter, M.K., Inokuma, M.S., Chiu, C.P., Harris, C.P., Waknitz, M.A., Itskovitz-Eldor, J., and Thomson, J.A. (2000). Clonally derived human embryonic stem cell lines maintain pluripotency and proliferative potential for prolonged periods of culture. Dev. Biol. *227*, 271–278.

Ananiev, G., Williams, E.C., Li, H., and Chang, Q. (2011). Isogenic pairs of wild type and mutant induced pluripotent stem cell (iPSC) lines from Rett syndrome patients as in vitro disease model. PLoS ONE *6*, e25255.

Anguera, M.C., Sadreyev, R., Zhang, Z., Szanto, A., Payer, B., Sheridan, S.D., Kwok, S., Haggarty, S.J., Sur, M., Alvarez, J., et al. (2012). Molecular signatures of human induced pluripotent stem cells highlight sex differences and cancer genes. Cell Stem Cell *11*, 75–90.

Bendall, S.C., Stewart, M.H., Menendez, P., George, D., Vijayaragavan, K., Werbowetski-Ogilvie, T., Ramos-Mejia, V., Rouleau, A., Yang, J., Bossé, M., et al. (2007). IGF and FGF cooperatively establish the regulatory stem cell niche of pluripotent human cells in vitro. Nature *448*, 1015–1021.

Boulting, G.L., Kiskinis, E., Croft, G.F., Amoroso, M.W., Oakley, D.H., Wainger, B.J., Williams, D.J., Kahler, D.J., Yamaki, M., Davidow, L., et al. (2011). A functionally characterized test set of human induced pluripotent stem cells. Nat. Biotechnol. *29*, 279–286.

Chan, E.M., Ratanasirintrawoot, S., Park, I.H., Manos, P.D., Loh, Y.H., Huo, H., Miller, J.D., Hartung, O., Rho, J., Ince, T.A., et al. (2009). Live cell imaging distinguishes bona fide human iPS cells from partially reprogrammed cells. Nat. Biotechnol. *27*, 1033–1037.

Cheung, A.Y., Horvath, L.M., Grafodatskaya, D., Pasceri, P., Weksberg, R., Hotta, A., Carrel, L., and Ellis, J. (2011). Isolation of MECP2-null Rett Syndrome patient hiPS cells and isogenic controls through X-chromosome inactivation. Hum. Mol. Genet. *20*, 2103–2115.

Chin, M.H., Mason, M.J., Xie, W., Volinia, S., Singer, M., Peterson, C., Ambartsumyan, G., Aimiuwu, O., Richter, L., Zhang, J., et al. (2009). Induced pluripotent stem cells and embryonic stem cells are distinguished by gene expression signatures. Cell Stem Cell *5*, 111–123.

de Napoles, M., Nesterova, T., and Brockdorff, N. (2007). Early loss of Xist RNA expression and inactive X chromosome associated chromatin modification in developing primordial germ cells. PLoS ONE *2*, e860.

Deuve, J.L., and Avner, P. (2011). The coupling of X-chromosome inactivation to pluripotency. Annu. Rev. Cell Dev. Biol. *27*, 611–629.

Diaz Perez, S.V., Kim, R., Li, Z., Marquez, V.E., Patel, S., Plath, K., and Clark, A.T. (2012). Derivation of new human embryonic stem cell lines reveals rapid epigenetic progression in vitro that can be prevented by chemical modification of chromatin. Hum. Mol. Genet. *21*, 751–764.

Dobyns, W.B., Filauro, A., Tomson, B.N., Chan, A.S., Ho, A.W., Ting, N.T., Oosterwijk, J.C., and Ober, C. (2004). Inheritance of most X-linked traits is not dominant or recessive, just X-linked. Am. J. Med. Genet. A. *129A*, 136–143.

Gontan, C., Achame, E.M., Demmers, J., Barakat, T.S., Rentmeester, E., van IJcken, W., Grootegoed, J.A., and Gribnau, J. (2012). RNF12 initiates X-chromosome inactivation by targeting REX1 for degradation. Nature *485*, 386–390.

Gore, A., Li, Z., Fung, H.L., Young, J.E., Agarwal, S., Antosiewicz-Bourget, J., Canto, I., Giorgetti, A., Israel, M.A., Kiskinis, E., et al. (2011). Somatic coding mutations in human induced pluripotent stem cells. Nature *471*, 63–67.

Hanna, J.H., Saha, K., and Jaenisch, R. (2010). Pluripotency and cellular reprogramming: facts, hypotheses, unresolved issues. Cell *143*, 508–525.

Hussein, S.M., Batada, N.N., Vuoristo, S., Ching, R.W., Autio, R., Närvä, E., Ng, S., Sourour, M., Hämäläinen, R., Olsson, C., et al. (2011). Copy number variation and selection during reprogramming to pluripotency. Nature *471*, 58–62.

Kim, K.Y., Hysolli, E., and Park, I.H. (2011). Neuronal maturation defect in induced pluripotent stem cells from patients with Rett syndrome. Proc. Natl. Acad. Sci. USA *108*, 14169–14174.

Kim, K.Y., Hysolli, E., and Park, I.H. (2012). Reprogramming human somatic cells into induced pluripotent stem cells (iPSCs) using retroviral vector with GFP. J. Vis. Exp., ().

Lengner, C.J., Gimelbrant, A.A., Erwin, J.A., Cheng, A.W., Guenther, M.G., Welstead, G.G., Alagappan, R., Frampton, G.M., Xu, P., Muffat, J., et al. (2010). Derivation of pre-X inactivation human embryonic stem cells under physiological oxygen concentrations. Cell *141*, 872–883.

Lessing, D., Anguera, M.C., and Lee, J.T. (2013). X chromosome inactivation and epigenetic responses to cellular reprogramming. Annu. Rev. Genomics Hum. Genet. *14*, 85–110.

Lister, R., Pelizzola, M., Kida, Y.S., Hawkins, R.D., Nery, J.R., Hon, G., Antosiewicz-Bourget, J., O'Malley, R., Castanon, R., Klugman, S., et al. (2011). Hotspots of aberrant epigenomic reprogramming in human induced pluripotent stem cells. Nature *471*, 68–73.

Maherali, N., Sridharan, R., Xie, W., Utikal, J., Eminli, S., Arnold, K., Stadtfeld, M., Yachechko, R., Tchieu, J., Jaenisch, R., et al. (2007). Directly reprogrammed fibroblasts show global epigenetic remodeling and widespread tissue contribution. Cell Stem Cell *1*, 55–70.

Mak, W., Nesterova, T.B., de Napoles, M., Appanah, R., Yamanaka, S., Otte, A.P., and Brockdorff, N. (2004). Reactivation of the paternal X chromosome in early mouse embryos. Science *303*, 666–669.

Marchetto, M.C., Carromeu, C., Acab, A., Yu, D., Yeo, G.W., Mu, Y., Chen, G., Gage, F.H., and Muotri, A.R. (2010). A model for neural development and treatment of Rett syndrome using human induced pluripotent stem cells. Cell *143*, 527–539.

Matsui, T., Leung, D., Miyashita, H., Maksakova, I.A., Miyachi, H., Kimura, H., Tachibana, M., Lorincz, M.C., and Shinkai, Y. (2010). Proviral silencing in embryonic stem cells requires the histone methyltransferase ESET. Nature *464*, 927–931.

Mekhoubad, S., Bock, C., de Boer, A.S., Kiskinis, E., Meissner, A., and Eggan, K. (2012). Erosion of dosage compensation impacts human iPSC disease modeling. Cell Stem Cell *10*, 595–609.

Navarro, P., Oldfield, A., Legoupi, J., Festuccia, N., Dubois, A., Attia, M., Schoorlemmer, J., Rougeulle, C., Chambers, I., and Avner, P. (2010). Molecular coupling of Tsix regulation and pluripotency. Nature *468*, 457–460.

Navarro, P., Moffat, M., Mullin, N.P., and Chambers, I. (2011). The X-inactivation trans-activator Rnf12 is negatively regulated by pluripotency factors in embryonic stem cells. Hum. Genet. *130*, 255–264.

Okamoto, I., Patrat, C., Thépot, D., Peynot, N., Fauque, P., Daniel, N., Diabangouaya, P., Wolf, J.P., Renard, J.P., Duranthon, V., and Heard, E. (2011). Eutherian mammals use diverse strategies to initiate X-chromosome inactivation during development. Nature *472*, 370–374.

Park, I.H., Arora, N., Huo, H., Maherali, N., Ahfeldt, T., Shimamura, A., Lensch, M.W., Cowan, C., Hochedlinger, K., and Daley, G.Q. (2008a). Disease-specific induced pluripotent stem cells. Cell *134*, 877–886.

Park, I.H., Zhao, R., West, J.A., Yabuuchi, A., Huo, H., Ince, T.A., Lerou, P.H., Lensch, M.W., and Daley, G.Q. (2008b). Reprogramming of human somatic cells to pluripotency with defined factors. Nature *451*, 141–146.

Plath, K., Fang, J., Mlynarczyk-Evans, S.K., Cao, R., Worringer, K.A., Wang, H., de la Cruz, C.C., Otte, A.P., Panning, B., and Zhang, Y. (2003). Role of histone H3 lysine 27 methylation in X inactivation. Science *300*, 131–135.

Pomp, O., Dreesen, O., Leong, D.F., Meller-Pomp, O., Tan, T.T., Zhou, F., and Colman, A. (2011). Unexpected X chromosome skewing during culture and reprogramming of human somatic cells can be alleviated by exogenous telomerase. Cell Stem Cell *9*, 156–165.

Shin, J., Bossenz, M., Chung, Y., Ma, H., Byron, M., Taniguchi-Ishigaki, N., Zhu, X., Jiao, B., Hall, L.L., Green, M.R., et al. (2010). Maternal Rnf12/RLIM is required for imprinted X-chromosome inactivation in mice. Nature *467*, 977–981.

Sugimoto, M., and Abe, K. (2007). X chromosome reactivation initiates in nascent primordial germ cells in mice. PLoS Genet. *3*, e116.

Takahashi, K., Tanabe, K., Ohnuki, M., Narita, M., Ichisaka, T., Tomoda, K., and Yamanaka, S. (2007). Induction of pluripotent stem cells from adult human fibroblasts by defined factors. Cell *131*, 861–872.

Tchieu, J., Kuoy, E., Chin, M.H., Trinh, H., Patterson, M., Sherman, S.P., Aimiuwu, O., Lindgren, A., Hakimian, S., Zack, J.A., et al. (2010). Female human iPSCs retain an inactive X chromosome. Cell Stem Cell *7*, 329–342.

Tomoda, K., Takahashi, K., Leung, K., Okada, A., Narita, M., Yamada, N.A., Eilertson, K.E., Tsang, P., Baba, S., White, M.P., et al. (2012). Derivation conditions impact X-inactivation status in female human induced pluripotent stem cells. Cell Stem Cell *11*, 91–99.

Wu, S.M., and Hochedlinger, K. (2011). Harnessing the potential of induced pluripotent stem cells for regenerative medicine. Nat. Cell Biol. *13*, 497–505.

Xu, R.H., Peck, R.M., Li, D.S., Feng, X., Ludwig, T., and Thomson, J.A. (2005). Basic FGF and suppression of BMP signaling sustain undifferentiated proliferation of human ES cells. Nat. Methods *2*, 185–190.

Yildirim, E., Kirby, J.E., Brown, D.E., Mercier, F.E., Sadreyev, R.I., Scadden, D.T., and Lee, J.T. (2013). Xist RNA is a potent suppressor of hematologic cancer in mice. Cell *152*, 727–742.

Yu, J., Vodyanik, M.A., Smuga-Otto, K., Antosiewicz-Bourget, J., Frane, J.L., Tian, S., Nie, J., Jonsdottir, G.A., Ruotti, V., Stewart, R., et al. (2007). Induced pluripotent stem cell lines derived from human somatic cells. Science *318*, 1917–1920.

Stem Cell Reports, Volume *2*

Supplemental Information

X Chromosome of Female Cells Shows Dynamic Changes in Status during Human Somatic Cell Reprogramming

Kun-Yong Kim, Eriona Hysolli, Yoshiaki Tanaka, Brandon Wang, Yong-Wook Jung, and In-Hyun Park

Supplemental Figure Legends

Figure S1. SNPs and qPCR analysis of secondary iPSC clones generated from fibroblast-like cells differentiated from mono-allelic iPSCs. (A) *GRPR* SNP in secondary iPSC clones derived from dfD551-iPSCK1 fibroblast cell lines showed that iPSC clones showing express the same or opposite allelic specificity as parental fibroblasts, both alleles are produced. **(B)** The expression levels of XCI related (*XIST*, *EZH2*, *RNF12*) and X linked genes (*MECP2*, *HPRT*) in mono- or bi-allelic iPSCs. Relative expressions are normalized against β-*ACTIN* and bars indicate mean ± S.E.M of three independent assays with three of mono-iPSC and bi-iPSC clones. Statistical significance was analyzed with Student's t-test; $^{*}p < 0.01$. **(C-E)** secondary iPSC clones isolated from fibroblast-like cell lines differentiated from mono-allelic RTT-iPSCs express MECP2 on X chromosome in a same or opposite allelic specificity as parental fibroblasts, or express from both alleles.

Figure S2. Decrease of XCI markers during the reprogramming. (A-C) Loss of H3K27me3 foci during reprogramming. RTT3, IMR90 and WI38 fibroblasts were reprogrammed and fixed at the given days. Cells were then stained for H3K27me3 (red) and DAPI (blue). GFP represents the expression of retrovirus-mediated reprogramming factors. Arrows indicate H3K27me3 foci. Scale bar: 20 μm. **(D)** Expression of XCI-related (*XIST*, *RNF12*) and pluripotent genes (*NANOG*, *LIN28a*, *REX1*) during reprogramming. **(E)** Change in expression of pluripotent genes (*LIN28a* and *REX1*) in cells isolated using a combination of markers given below at different reprogramming stages. Relative expression of the given genes was calculated by normalized against β-*ACTIN* after qPCR. Error bars represent mean ± SD in triplicate reactions.

Figure S3. Analysis of X chromosome status in secondary iPSCs derived from LNS-syndrome fibroblasts with a mutation in *HPRT*. (A) Stable maintenance of inactive X

chromosome after drug selection. HAT-(fLNS-HAT) or 6TG-(fLNS-6TG) selected LNS fibroblasts were cultured with drugs for two weeks, and cultured with either drug. fLNS-HAT cells do not show resistance ot 6TG, and fLNS-6TG cells do not show resistance to HAT. **(B)** *GYG2* SNP analysis of secondary iPSC lines derived from df6TG-3($Xa^{HPRT-}Xi^{HPRT+}$) that was differentiated from 6TG-iPSC3 having 6TG-resistance and (C) SNP in *GYG2*. Secondary iPSC clones with C, T, or C/T SNPs were isolated, showing the generation of iPSC with X chromosome state converted. **(C)** Drug resistance of iPSC clones derived from fLNS-HAT ($Xa^{HPRT+}Xi^{HPRT-}$) that has an A SNP in *MAOA* gene on X chromosome. Clones with resistance to HAT (HAT-iPSC1) or to 6TG (HAT-iPSC2) were generated. The corresponding SNP in *MAOA* gene is shown in left column. Among HAT-resistant clones, iPSC clones with two active X chromosomes were isolated (HAT-iPSC5). Crystal violet staining was performed in iPSCs after HAT or 6TG selection for 14 days. **(D)** Drug resistance of secondary iPSCs derived from fibroblast-like cells (dfHAT-iPSC1, $Xa^{HPRT+}Xi^{HPRT-}$) differentiated from HAT-iPSC1 that is resistant to HAT. secondary iPSC clones resistant to HAT, or 6TG were isolated. Crystal violet staining of secondary iPSCs was performed after 14 days of drug selection. **(E)** SNP analysis of *GYG2* and *MAOA* genes present on X chromosome in secondary iPSCs derived from dfHAT-1. **(F)** Representative H3K27me3/OCT4 staining images of secondary iPSC derived from dfHAT-1. Secondary dHAT1-iPSC2 that is resistant to 6TG has H3K27me3 foci, while secondary dHAT1-iPSC6 expresses both alleles of *GYG2* and *MAOA* and has no H3K27me3 foci. Scale bar: 20 μm. **(G)** Southern blot analysis to identify the integration of provirus. Genomic DNA from each of 6TG-iPSC clones derived from 6TG selected fibroblasts were digested with EcoRI and SpeI, and hybrizided with *GFP*, *OCT4* and *SOX2* probes.

Figure S4. Tracing X chromosome status in nascent iPSC clones. (A) Representative images of H3K27me3/OCT4 staining with iPSC clones at the given passages. After picked up and passaged, RTT3-iPSC11 clone maintains the inactive X chromosome marker H3K27me3, while RTT3-iPSC13 clone loses the marker. White rectangular boxes on the upper right corner of RTT3-iPSC13 figures represent the magnified images of cellular border showing the presence and absence of H3K27me3 foci. Nuclei were counterstained with DAPI (blue). Scale bar: 20 μm. **(B)** Magnified images of H3K27me3 staining with Detroit-iPSCN1 clones at passages 2 and 3 as related with Figure 4A. White dotted line indicates the boundary between H3K27me3 foci positive and negative area. **(C)** FISH analysis for *XIST* RNA in mono-allelic RTT3-iPS11and bi-allelic RTT3-iPS13 clone at passages 10 and 12. Scale bar: 10 um. **(D-F)** Quantification of the percentage of established iPSC clones showing H3K27me3 foci-negative cells during passages as shown in Figure S4A. A total of ten RTT3-iPSCs, six HAT-iPSCs and six 6TG-iPSC clones were picked and expanded to trace the change of H3K27me3 status. Black, H3K27me3 foci-positive clones; Dark gray, clones mixed with H3K27me3 foci-positive and negative cells; Light gray, H3K27me3 foci-negative clones.

Figure S5. Gain of H3K27me3 foci in differentiated cells undergone XCI and a model of change in X chromosome status. (A) Induction of XCI-linked *RNF12* and concurrent decrease of pluripotency markers in cells differentiated from bi-allelic iPSC clones. Mono-allelic cells and H1 (ESCs) were used for control. β–*ACTIN* was used to normalize the changes in triplicate reactions. **(B)** Appearance of H3K27me3 foci-positive cells in fibroblast-likes cells differentiated from IMR-iPSC3 and RTT3-iPSC43 iPSC clones having no H3K27me3 foci. 6TG-iPSC6 cells do not show H3K27me3 foci after differentiation, suggesting that they are Class III iPSC. Arrows indicate H3K27me3 foci. Scale bar: 20 μm. **(C)** SNPs and analysis of iPSC clones

generated from 6TG drug selected fLNS-6TG cells. **(D)** Modeling showing the dynamics in X chromosome status in human somatic cell reprogramming. In addition to previously shown retention of the inactive X chromosome (XCI retention), here we showed that the inactive X chromosome becomes re-activated by overexpression of reprogramming factors (rXCR, reprogramming-XCR), marked by repression of XCI-genes (*XIST*, *RNF12*), loss of H3K27me3 foci and expression of genes that are located in the inactive X chromosome. Completion of reprogramming induces a random XCI. In some established iPSC clones, iPSC clones without the inactive X chromosome marks arise that include Class I iPSC having two active X chromosomes as well as Class III iPSCs having on active and one eroded X chromosome.

Figure S1

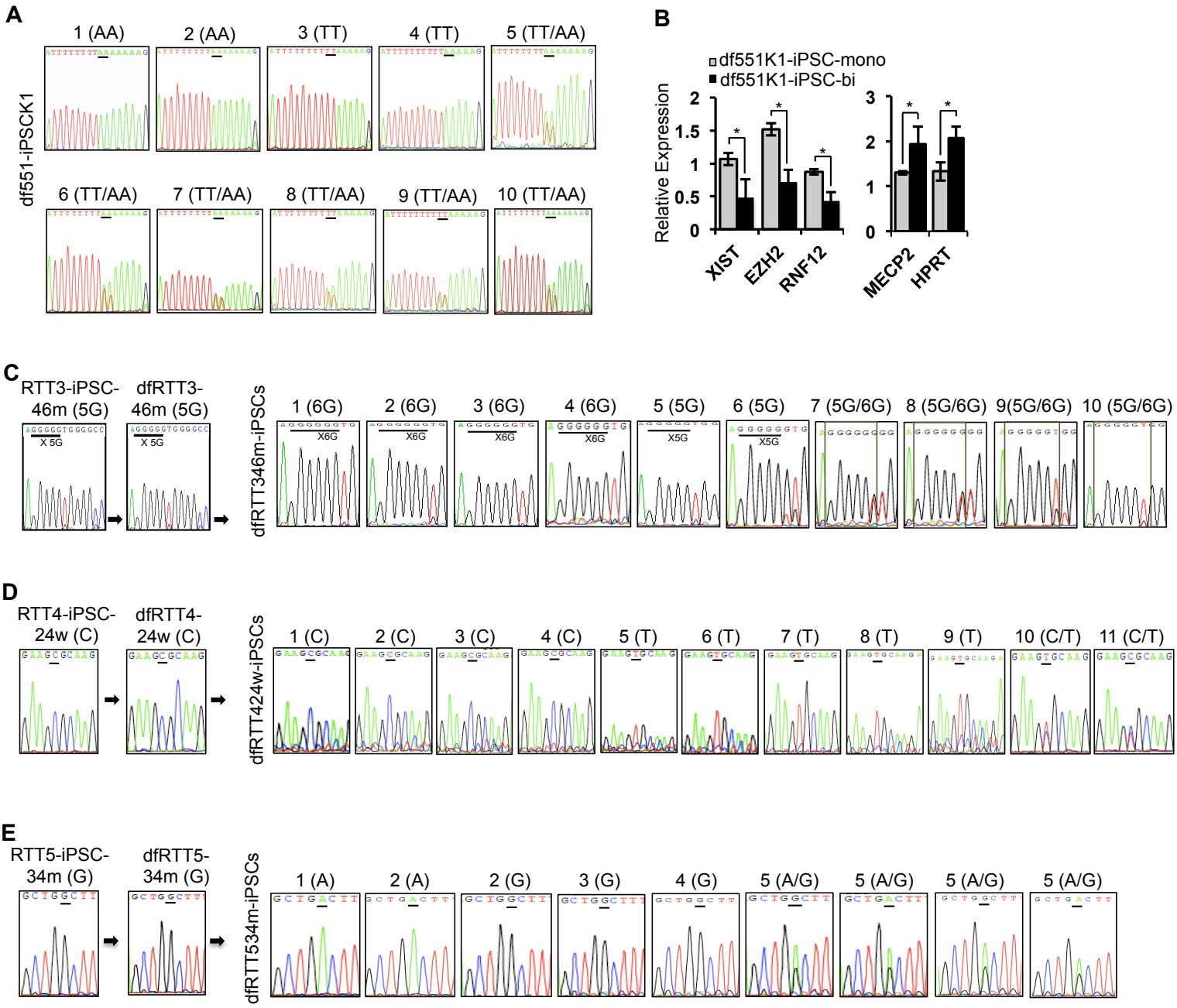
A
1 (AA)
2 (AA)
3 (TT)
4 (TT)
5 (TT/AA)
df551-iPSCK1
6 (TT/AA)
7 (TT/AA)
8 (TT/AA)
9 (TT/AA)
10 (TT/AA)
B
df551K1-iPSC-mono
df551K1-iPSC-bi
Relative Expression
XIST
EZH2
RNF12
MECP2
HPRT
C
RTT3-iPSC-46m (5G)
dfRTT3-46m (5G)
dfRTT346m-iPSCs
1 (6G)
2 (6G)
3 (6G)
4 (6G)
5 (5G)
6 (5G)
7 (5G/6G)
8 (5G/6G)
9(5G/6G)
10 (5G/6G)
D
RTT4-iPSC-24w (C)
dfRTT4-24w (C)
dfRTT424w-iPSCs
1 (C)
2 (C)
3 (C)
4 (C)
5 (T)
6 (T)
7 (T)
8 (T)
9 (T)
10 (C/T)
11 (C/T)
E
RTT5-iPSC-34m (G)
dfRTT5-34m (G)
dfRTT534m-iPSCs
1 (A)
2 (A)
2 (G)
3 (G)
4 (G)
5 (A/G)
5 (A/G)
5 (A/G)
5 (A/G)

Figure S2

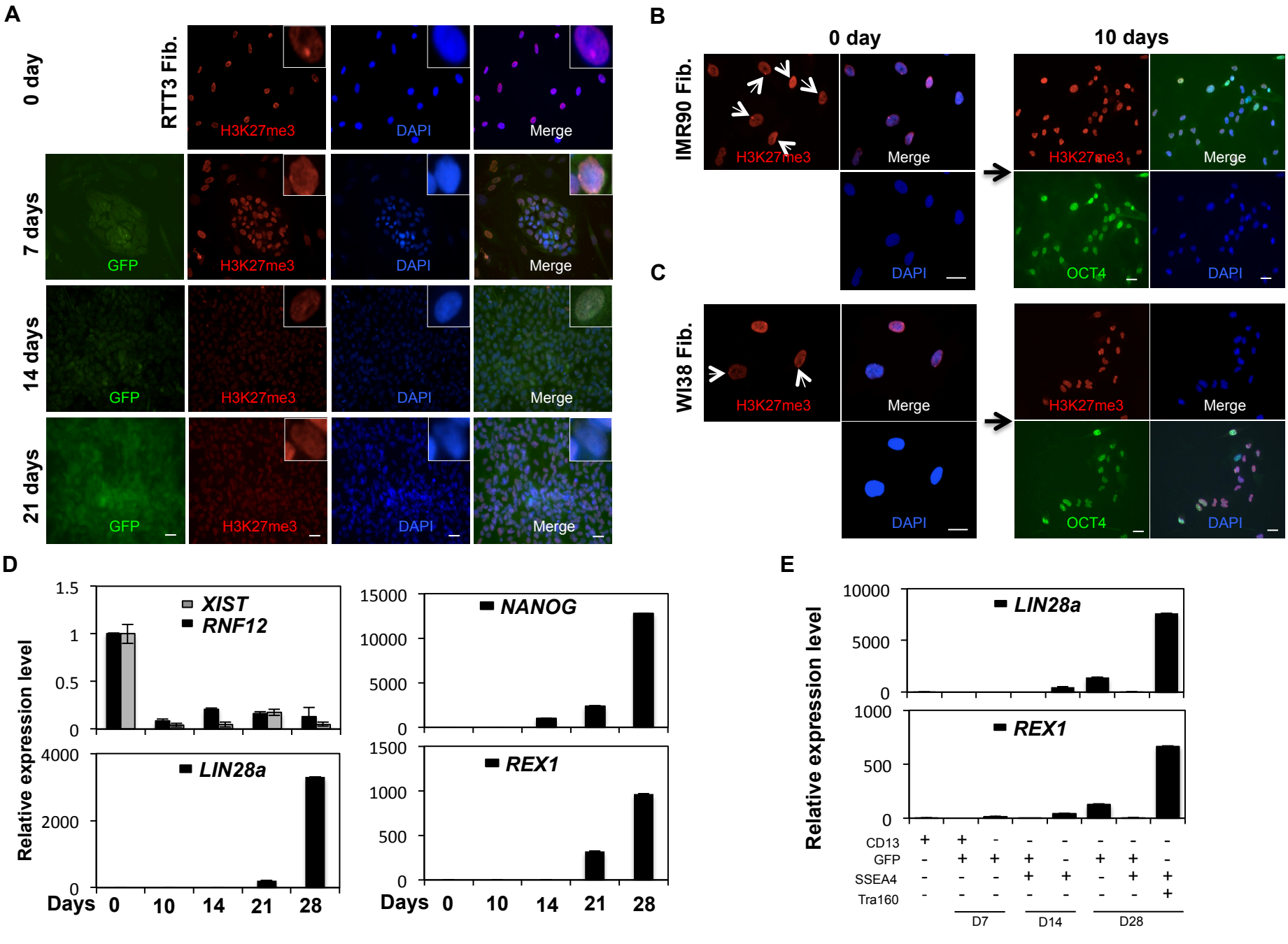
A
0 day
RTT3 Fib.
H3K27me3
DAPI
Merge
7 days
GFP
14 days
21 days
B
0 day
10 days
IMR90 Fib.
OCT4
C
WI38 Fib.
D
XIST
RNF12
NANOG
LIN28a
REX1
Relative expression level
Days 0 10 14 21 28
E
CD13
GFP
SSEA4
Tra160
D7
D14
D28

Figure S3

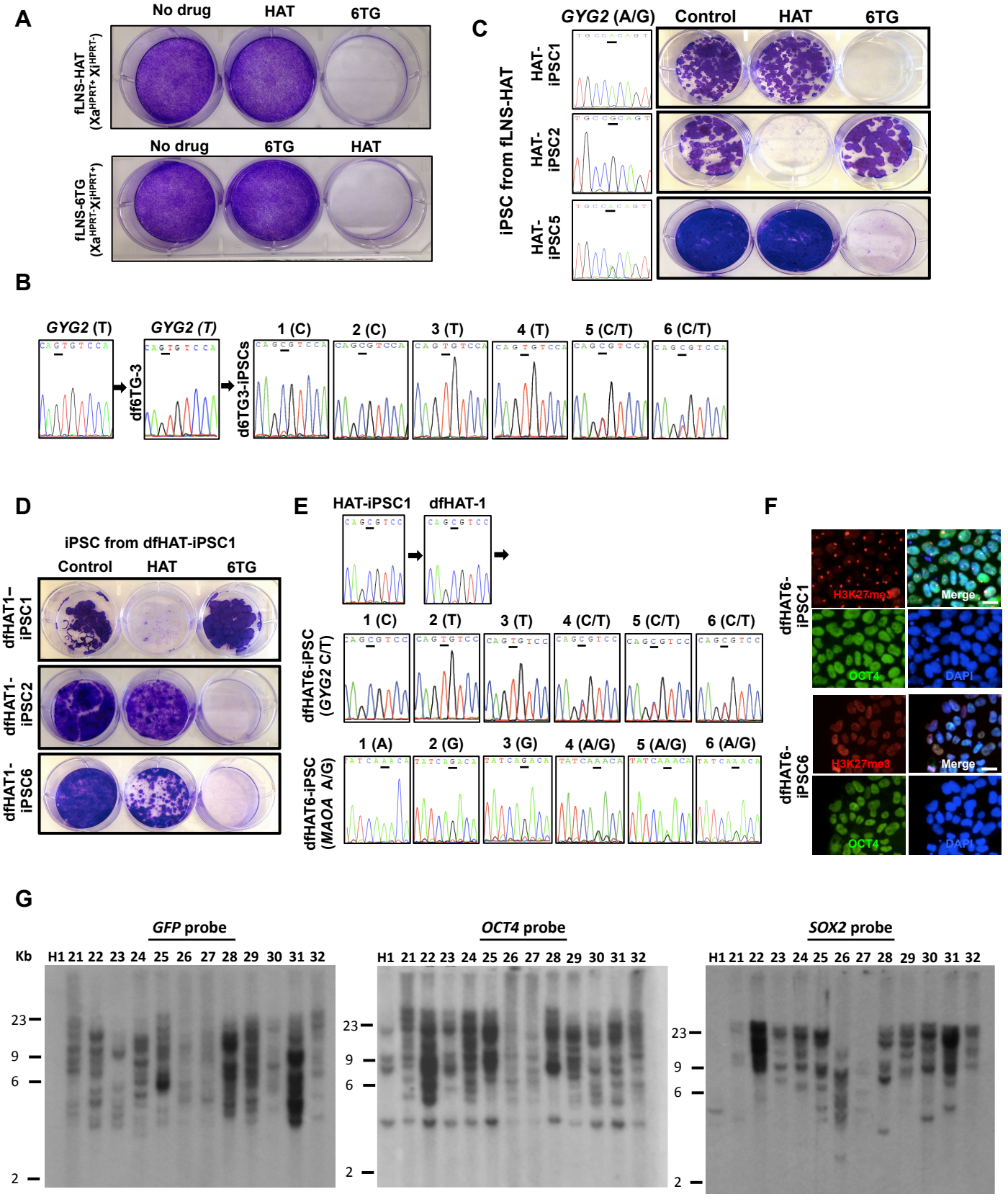
A
No drug
HAT
6TG
fLNS-HAT
(Xa^HPRT+ Xi^HPRT-)
No drug
6TG
HAT
fLNS-6TG
(Xa^HPRT- Xi^HPRT+)
B
GYG2 (T)
GYG2 (T)
df6TG-3
d6TG3-iPSCs
1 (C)
2 (C)
3 (T)
4 (T)
5 (C/T)
6 (C/T)
C
GYG2 (A/G)
Control
HAT
6TG
iPSC from fLNS-HAT
HAT-iPSC1
HAT-iPSC2
HAT-iPSC5
D
iPSC from dfHAT-iPSC1
Control
HAT
6TG
dfHAT1–iPSC1
dfHAT1-iPSC2
dfHAT1-iPSC6
E
HAT-iPSC1
dfHAT-1
1 (C)
2 (T)
3 (T)
4 (C/T)
5 (C/T)
6 (C/T)
dfHAT6-iPSC (GYG2 C/T)
1 (A)
2 (G)
3 (G)
4 (A/G)
5 (A/G)
6 (A/G)
dfHAT6-iPSC (MAOA A/G)
F
dfHAT6-iPSC1
H3K27me3
Merge
OCT4
DAPI
dfHAT6-iPSC6
H3K27me3
Merge
OCT4
DAPI
G
GFP probe
OCT4 probe
SOX2 probe
Kb
H1 21 22 23 24 25 26 27 28 29 30 31 32
23
9
6
2

Figure S4

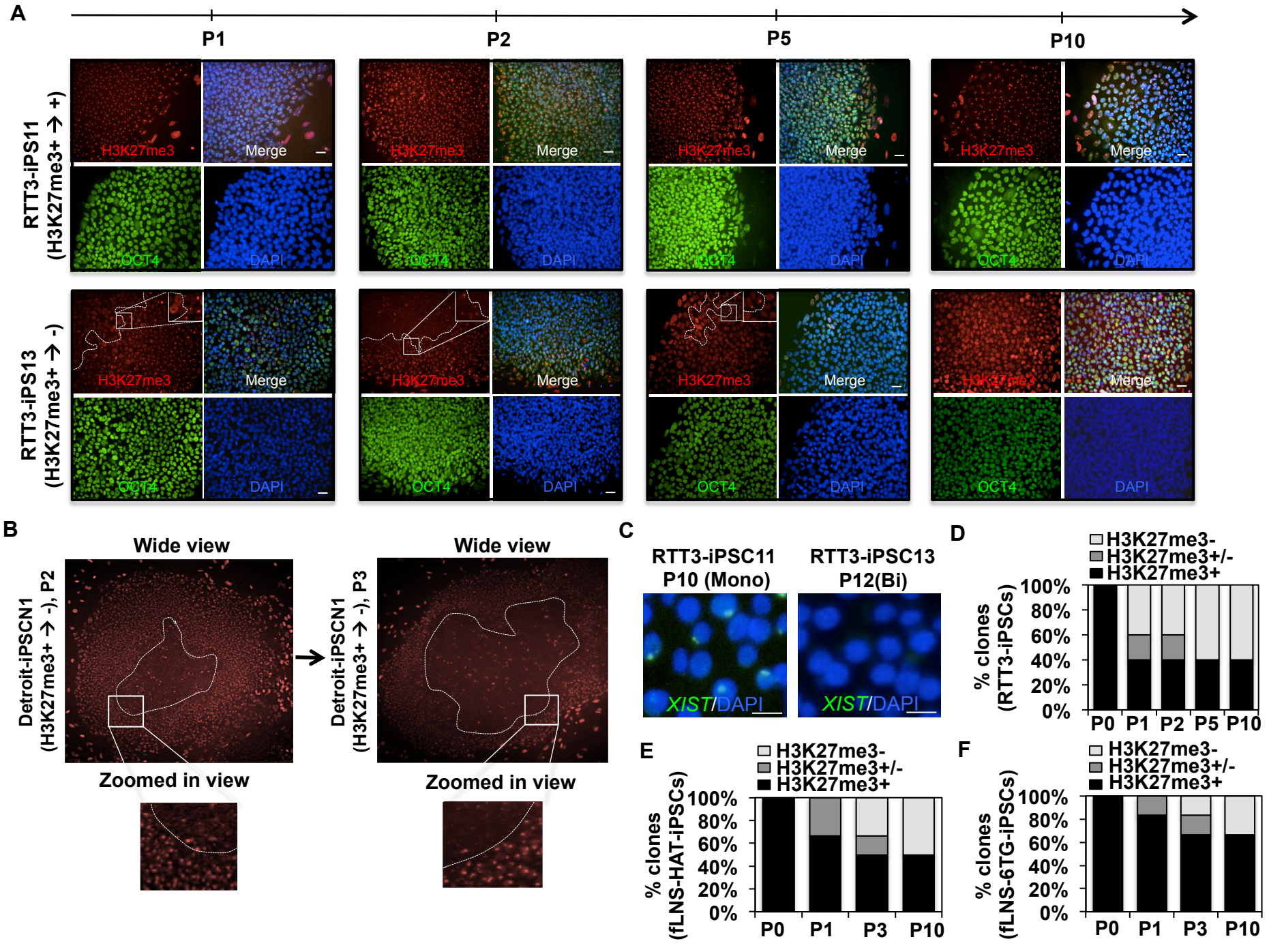
A
P1
P2
P5
P10
RTT3-iPS11
(H3K27me3+ → +)
RTT3-iPS13
(H3K27me3+ → -)
H3K27me3
Merge
OCT4
DAPI
B
Wide view
Detroit-iPSCN1
(H3K27me3+ → -), P2
Detroit-iPSCN1
(H3K27me3+ → -), P3
Zoomed in view
C
RTT3-iPSC11
P10 (Mono)
RTT3-iPSC13
P12(Bi)
XIST/DAPI
D
H3K27me3-
H3K27me3+/-
H3K27me3+
% clones
(RTT3-iPSCs)
100%
80%
60%
40%
20%
0%
P0
P1
P2
P5
P10
E
% clones
(fLNS-HAT-iPSCs)
P0
P1
P3
P10
F
% clones
(fLNS-6TG-iPSCs)
P0
P1
P3
P10

Figure S5

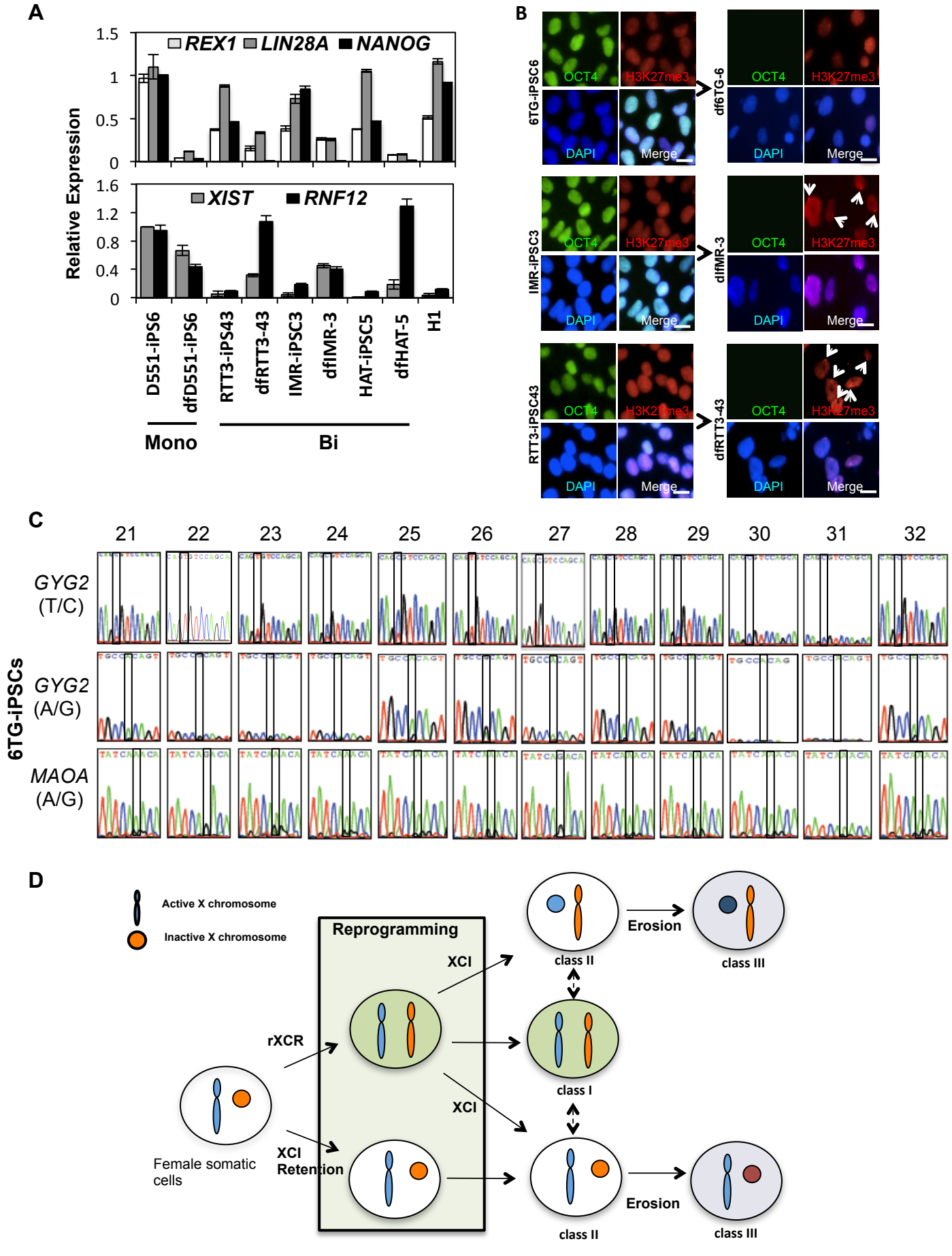
A
REX1
LIN28A
NANOG
XIST
RNF12
Relative Expression
D551-iPS6
dfD551-iPS6
RTT3-iPS43
dfRTT3-43
IMR-iPSC3
dfIMR-3
HAT-iPSC5
dfHAT-5
H1
Mono
Bi
B
6TG-iPSC6
df6TG-6
IMR-iPSC3
dfIMR-3
RTT3-iPSC43
dfRTT3-43
OCT4
H3K27me3
DAPI
Merge
C
6TG-iPSCs
GYG2 (T/C)
GYG2 (A/G)
MAOA (A/G)
21
22
23
24
25
26
27
28
29
30
31
32
D
Active X chromosome
Inactive X chromosome
Reprogramming
XCI
rXCR
XCI
XCI Retention
Female somatic cells
class II
Erosion
class III
class I
class II
Erosion
class III

Table S1. List of primers used for RT-qPCR

Gene	Forward	Reverse
MECP2	CCAGGACTTGAGCAGCAGCG	CGGGAAGCTTTGTCAGAGCCC
XIST	CGGTACGTTGAAGTTAGGGAATG	GTGCTGTATAATCCAATGGGTAG
EZH2	ACCGGTTGTGGGCTGCACAC	TGCAGCGGCATCCCGGAAAG
RNF12	ACCGATTGGATCGAGAAGAAGC	TGTAGTCGTCTCAGCAACTCT
NANOG	TGAACCTCAGCTACAAACAG	TGGTGGTAGGAAGAGTAAAG
REX1	GCGTCATAAGGGGTGAGTTTT	AGAACATTCAAGGGAGCTTGC
ACTIN	TGAAGTGTGACGTGGACATC	GGAGGAGCAATGATCTTGAT
***OCT4* total**	AGCGAACCAGTATCGAGAAC	TTACAGAACCACACTCGGAC
***OCT4* endo**	CCTCACTTCACTGCACTGTA	CAGGTTTTCTTTCCCTAGCT
***OCT4* ecto**	CCTCACTTCACTGCACTGTA	CCTTGAGGTACCAGAGATCT
***SOX2* total**	AGCTACAGCATGATGCAGGA	GGTCATGGAGTTGTACTGCA
***SOX2* endo**	CCCAGCAGACTTCACATGT	CCTCCCATTTCCCTCGTTTT
***SOX2* ecto**	CCCAGCAGACTTCACATGT	CCTTGAGGTACCAGAGATCT
***MYC* total**	ACTCTGAGGAGGAACAAGAA	TGGAGACGTGGCACCTCTT
***MYC* endo**	TGCCTCAAATTGGACTTTGG	GATTGAAATTCTGTGTAACTGC
***MYC* ecto**	TGCCTCAAATTGGACTTTGG	CGCTCGAGGTTAACGAATT
***KLF4* total**	TCTCAAGGCACACCTGCGAA	TAGTGCCTGGTCAGTTCATC
***KLF4* endo**	GATGAACTGACCAGGCACTA	GTGGGTCATATCCACTGTCT
***KLF4* ecto**	GATGAACTGACCAGGCACTA	CCTTGAGGTACCAGAGATCT

Table S2. List of primers used for allelic expression and for probe for Southern Blot

Gene	Forward	Reverse
MECP2 for RTT3 RTT4	AGGTAGGCGACACATCCCT	CTTACAGGTCTTCAGGACCTT
MECP2 for RTT5	AGAAACGGGGCCGAAAGCCG	CGGGAAGCTTTGTCAGAGCC
GRPR	AGCCCTGTTAAATGGTCGTG GCC	ATGGTGGAATGGCACCCTGGATGA
HPRT	TGTGGCCATCTGCCTAGTAA	CAGCCAACACTGCTGAAACA
GYG2	CAGCACGCCATGGAACACGGCA	AGGCTGAATCCGCAC ACGG CC
MAOA	ACTCCCTGCTTAGCTCTGTGGG	GTGGGCACCCTTGTGGGCCGAC
GFP **probe**	GGTGAGCAAGGGCGAGGAGC	CAGGGTGTCGCCCTCGAACTTC
OCT4 **probe**	TGGAGGTGATGGGCCAGG	CCGGGTTTTGCTCCAGCT
SOX2 **probe**	GGCCCGCAGCAAACTTCG	GGGCCAGCAGCCCGCCGG

Supplemental Experimental Procedures

Cell Culture and Reprogramming.

Reprogramming was performed as previously described (Kim et al., 2011). In short, retrovirus expressing OCT4, SOX2, KLF4 and c-MYC were generated in 293T cells by transfecting 0.25 ug VSVG, 2.25 ug GAG-POL, and 2.5 ug pMIG vector expressing each of four genes in 10 cm plate. X-tremeGENE 9 (Roche) was used for transfection following manufacturer's instruction. 1 x 10^5 cells in one well of 6-well plate were infected with retrovirus expressing reprograming factors with MOI=5 in the presence of 10 ug/ml protamine sulfate. Five days after infection, cells were plated on irradiated MEFs and replenished with human ESC medium every day. When were formed, iPSCs were picked up by 10 uL Pipetman onto plate pre-plated with MEFs and maintained according to standard protocol (Park et al., 2008).

Isolation of cells undergoing reprogramming

Following reprogramming with pMIG retrovirus expressing reprogramming factors, cells were harvested at day 7, 14, and 28 by treating with accutase. Cells at 7 days after reprogramming were stained in FACS buffer (1% FBS in 1XPBS) for 30 minutes at 4°C with antibodies recognizing CD13 (BD Pharmigen cat# 555394), and SSEA4 (R&D cat# FAB1435A). Cells at 14 days and 28 days after reprogramming were stained for CD13 (BD Pharmigen cat# 555394), SSEA4 and TRA160 (BD Pharmigen cat# 560193). Stained cells were sorted according to the combined expression of cell surface markers and retroviral GFP expression using Yale Stem Cell Center FACS Core.

Gene Expression and SNP Analysis

Gene expression analysis was performed with real-time PCR using iQSYBR Green Supermix (BioRad) with primers listed in Table S1. The data were analyzed by using comparative threshold cycle (CT) method and normalized to β-*ACTIN*. All qPCR assays were performed in

triplicates. To identify SNPs, X-linked *GRPR*, *MAOA*, *GYG2* and *MECP2* genes were amplified from cDNA by PCR using primers in Table S2 and subjected to Sanger sequencing using the Keck DNA Sequencing Facility at Yale School of Medicine or restriction digestion.

Immunostaining

iPSCs, or cells undergoing reprogramming were fixed for 10 min at room temperature with 4% paraformaldehyde in PBS, and permeabilized by using 0.2% Triton X-100 in PBS for 5 min. After blocking with 3% BSA blocking buffer in PBS, cells were incubated with primary antibodies for OCT4 (Ab19857, Abcam), H3K27me3 (#9733, Cell Signaling Technologies), and/or MECP2 (C-17, Santa Cruz) for 2hr at RT or overnight at 4 °C in blocking solution. Cells were then incubated with Alexa-488 (A11008, Invitrogen) and Alexa-546 (A21422, Invitrogen) labeled secondary antibodies and stained with DAPI.

FISH for *XIST* and *ATRX*

RNA FISH was carried out as described previously (Tchieu et al., 2010). Briefly, iPSCs were on gelatin coated coverslips and permeabilized by means of sequential transfer into twice ice-cold PBS for 30 sec, ice-cold CSK buffer (100mM NaCl, 300 mM sucrose, 3mM MgCl2 and 10 mM pH 6.8 PIPES and RNase-inhibitor RNasin) for 30 sec, and then CSK buffer containing 0.2% Triton X-100 buffer for 15 min, followed twice with CSK buffer for 30 sec each. Cells were then fixed with 4% formaldehyde in PBS for 15 min and dehydrated through sequential changes of 70%, 85% 95% and 100% EtOH for 3 min each, followed by air drying before hybridization of *XIST* and *ATRX* probe. For the *XIST* and *ATRX* probe, double-strand shorter DNA probes were generated form G1A plasmid (Clemson et al., 1996) and BACs (RP11-1145J4 and RP11-42M11). Probes were labeled with fluorescein-12-dUTP using the Prime-It Fluor Labeling kit (Stratagene). The probe was then hybridized with the prepared sample at 37 °C overnight in a humidified chamber.

Western Blot

Cells were lysed directly in RIPA lysis buffer (20 mM pH 7.5 Tris-HCl, 150 mM NaCl, 1 mM Na2EDTA, 1 mM EGTA, 1% NP-40, 1% sodium deoxycholate and protease inhibitor cocktail) and western blot analysis was performed with antibody recognizing the C-terminus of MECP2 (C-17, Santa Cruz). β-ACTIN was used as loading control.

Southern Blot

The genomic DNA was isolated from individual iPSC clones according to the method previously published (Laird et al., 1991). Total 5 μg of genomic DNA was digested overnight with EcoRI and SpeI according to a standard protocol, separated in 0.8% gel, and transferred to Nylon membrane. *GFP, OCT4* and *SOX2* probes were generated by performing PCR in pMSCV vectors using primers listed on Table S2. PCR products were purified using Qiagen PCR purification kit and labeled with α-^{32P}-dCTP according to the Prime-it II random primer labeling kit manual (Agilent). Blots were hybridized (MyracleHyb, Stratagene) overnight to detect the presence of the integrated provirus encoding *GFP, OCT4*, or *SOX2.*

SUPPLEMENTAL REFERENCES

Clemson, C.M., McNeil, J.A., Willard, H.F., and Lawrence, J.B. (1996). XIST RNA paints the inactive X chromosome at interphase: evidence for a novel RNA involved in nuclear/chromosome structure. J Cell Biol *132*, 259-275.

Kim, K.Y., Hysolli, E., and Park, I.H. (2011). Neuronal maturation defect in induced pluripotent stem cells from patients with Rett syndrome. Proceedings of the National Academy of Sciences of the United States of America *108*, 14169-14174.

Laird, P.W., Zijderveld, A., Linders, K., Rudnicki, M.A., Jaenisch, R., and Berns, A. (1991). Simplified mammalian DNA isolation procedure. Nucleic Acids Res *19*, 4293.

Park, I.H., Lerou, P.H., Zhao, R., Huo, H., and Daley, G.Q. (2008). Generation of human-induced pluripotent stem cells. Nat Protoc *3*, 1180-1186.

Tchieu, J., Kuoy, E., Chin, M.H., Trinh, H., Patterson, M., Sherman, S.P., Aimiuwu, O., Lindgren, A., Hakimian, S., Zack, J.A.*, et al.* (2010). Female human iPSCs retain an inactive X chromosome. Cell Stem Cell *7*, 329-342.